

CHARGED HEAVY LEPTON PRODUCTION IN SUPERSTRING INSPIRED E6 MODELS

M.M. BOYCE, M.A. DONCHESKI

*Carleton University, Physics Department, 1125 Colonel By Drive, Ottawa,
Ontario, K1S 5B6, Canada*

H. KÖNIG

*UQAM, Département de Physique, CP 8888, Succ. Centre Ville, Montréal,
Québec, H3C 3P8, Canada*

Abstract

The possibility of studying superstring inspired E_6 phenomenology at high energy hadron colliders is investigated. A very simple low energy rank-5 Supersymmetric (N=1) model is considered, which consists of three scalar-Higgses, $H_{i=1,2,3}^0$, two charged-Higgses, H^\pm , one pseudo-scalar-Higgses, P^0 , and an extra vector boson, the Z' . The production of charged heavy leptons pairs, L^+L^- , by gluon-gluon fusion and Drell-Yan mechanisms is discussed. For gluon-gluon fusion an enhancement in the parton level cross-section is expected due to the heavy (s)fermion loops which couple to the gluons. This mechanism is expected to dominate over Drell-Yan for L^+L^- invariant masses above the Z' mass.

I. INTRODUCTION

In this paper the production of charged heavy leptons pairs, L^+L^- , *via* superstring inspired E_6 models, at high energy hadron colliders will be investigated [1,2]. A general overview of E_6 models will be presented in which several simplifying assumptions will be made in order to restrict the L^+L^- production computation to a manageable one. In particular, a low energy rank-5 model, arising from E_6 , will be constructed, with this specific application in mind. The L^+L^- production cross-sections will then be computed followed by a discussion and then finally conclusions.

Many aspects of the rank-5 models, that will be considered here, are covered in the literature. Unfortunately, when trying to extract the particular model dependent information, needed for L^+L^- production, it appeared that the existing literature was not consistent. Therefore, it was felt that in order to avoid any ambiguities that the model should be carefully reconstructed from the ground up. When constructing the model careful attention was paid to being as consistent as possible with the literature concerning: factors of two, hypercharge conventions, signs, ambiguous notational subtleties, etc. Much of the analysis of the model was done by using Mathematica [3] to generate the various couplings, mass matrices, etc., directly from the superpotential. This enabled easy comparison with various literature sources [4–9]. Differing conventions and normalizations aside, the most significant problem arose with the charged-Higgs, Eq. (38), and pseudo-scalar-Higgs, Eq. (39), mass terms; a factor two was missing in front of the $\sin\beta\cos\beta$ terms, *op. cit.* For example, in the case of the pseudo-scalar-Higgs the aforementioned authors disagree to by an overall factor of two in their mass-mixing matrices but not in their eigenvalues. As a result, the analysis of the mass constraints in the Higgs sector [9] had to be re-evaluated, Figs. 6-9. In addition Appendix A contains a summary of the couplings used for L^+L^- production which, in general, could not be obtained from the literature.

II. SUPERSTRING INSPIRED E_6 MODELS

The $SU(3)_c \otimes SU(2)_L \otimes U(1)_Y$ standard model (SM) is a very successful model [10]. It has thus far withstood a lot of rigorous experimental testing; however, despite its success the SM has many of problems:

- no unification of the forces
- gauge hierarchical and fine tuning problems
- three generations of quarks and leptons for no particular reason
- too many parameters to be extracted from experiment

Some of the earlier attempts at unification tried to unify the strong and electroweak forces by embedding the $SU(3)_c \otimes SU(2)_L \otimes U(1)_Y$ structure into higher groups, such as $SU(5)$ and $SO(10)$. These “grand unified theories” [11], or GUT’s, were only partially successful. The simplest of the GUT’s was $SU(5)$ which seemed promising at the time because it predicted the ratio of the $SU(2)_w$ and $U(1)_{em}$ couplings and the proton lifetime [12]. However, the ordinary $SU(5)$ GUT is no longer a possibility because more refined experimental measurements are now in disagreement with its predictions for the couplings and the proton lifetime [4]. In addition this simple model had too many parameters and no explanation for family replication. The next likely candidate group was $SO(10)$ [13], although the three (or more) copies of the generational structure still had to be inserted by hand.

Difficulties with the SM and GUT models concerning gauge hierarchy and fine tuning problems led to theoretical remedies such as technicolour and supersymmetry (SUSY) [14]. The most appealing of these theories was SUSY [15], which had generators that related particles of different spin in the same supermultiplet. The locality of these generators leads to supergravity models. SUSY (and its extended versions) however, did not have enough room for all of the SM particles [12]. To solve this problem direct product structures were

made with SUSY and Yang-Mills gauge groups. These structures are now commonly referred to as “SUSY” models [16,17]. Of course the price paid for this was a large particle spectrum (at least twice that of the SM) and the problem of family replication still remained.

In the early 1970’s some interest was sparked in E_6 as a GUT when it was discovered that all the then known generations of fermions could be placed in a single **27** dimensional representation. This (“topless”) model [18] was quite popular because the newly discovered τ lepton and b quark could also be fitted neatly into the **27**; there was no need for a third generation. However this model was quickly disallowed, as it was experimentally [18] shown that the τ and b belonged to a third generation, and the idea of E_6 as a GUT died.

$$\begin{aligned}
\mathbf{27} &= \left\{ \left[\begin{array}{cc} \begin{pmatrix} u \\ d \end{pmatrix}_L & \begin{pmatrix} \nu_e \\ e \end{pmatrix}_L \\ u_L^c d_L^c e_L^c & \nu_{eL}^c d_L^c d_L^c \end{array} \right] \begin{pmatrix} \nu'_e \\ e' \end{pmatrix}_L \begin{pmatrix} e' \\ \nu'_e \end{pmatrix}_L^c \nu_{eL}^c \right\} \\
\mathbf{27} &= \left\{ \left[\begin{array}{cc} \begin{pmatrix} c \\ s \end{pmatrix}_L & \begin{pmatrix} \nu_\mu \\ \mu \end{pmatrix}_L \\ c_L^c s_L^c \mu_L^c & \nu_{\mu L}^c s_L^c s_L^c \end{array} \right] \begin{pmatrix} \nu'_\mu \\ \mu' \end{pmatrix}_L \begin{pmatrix} \mu' \\ \nu'_\mu \end{pmatrix}_L^c \nu_{\mu L}^c \right\} \\
\mathbf{27} &= \left\{ \left[\begin{array}{cc} \begin{pmatrix} t \\ b \end{pmatrix}_L & \begin{pmatrix} \nu_\tau \\ \tau \end{pmatrix}_L \\ t_L^c b_L^c \tau_L^c & \nu_{\tau L}^c b_L^c b_L^c \end{array} \right] \begin{pmatrix} \nu'_\tau \\ \tau' \end{pmatrix}_L \begin{pmatrix} \tau' \\ \nu'_\tau \end{pmatrix}_L^c \nu_{\tau L}^c \right\}
\end{aligned}$$

FIG. 1. E_6 particle content.^a The SM particles are shown in the boxes on the left and their “exotic” counterparts outside the boxes on the right. Although the exotics are labeled in away that suggests they have the same quantum numbers as the non-exotics, in general they need not. The labeling for these particles in the literature has not been settled upon and varies quite significantly from paper to paper [4]. Here the labeling scheme was chosen to reflect a specific E_6 model that will be constructed in this paper. In particular, all the exotics will carry the “expected” quantum numbers as their non-exotic counter parts do, with the exception being $L=0$ for the primed and double primed ones.

^aNote: Embedded in the **27**’s is the symmetry group $SU(2)_I$ [4] due to an ambiguity in the particle assignments $\left\{ \begin{pmatrix} \nu_l \\ l \end{pmatrix}_L, a_L^c \right\} \Leftrightarrow \left\{ \begin{pmatrix} \nu'_l \\ l' \end{pmatrix}_L, a_L^c \right\}$ and $\{\nu_{lL}^c\} \Leftrightarrow \{\nu_{lL}^c\}$ [cf. Fig. 2(d)]. This ambiguity can easily be seen via the decomposition $\mathbf{27} = \sum_{\oplus} (\text{SO}(10), \text{SU}(5))$.

In late 1984 Green and Schwarz [19] showed that 10 dimensional string theory is anomaly free if its gauge group is either $E_8 \otimes E'_8$ or $SO(32)$. The group that had received the most attention was $E_8 \otimes E'_8$ as it led to chiral fermions, similar to those in the SM, whereas $SO(32)$ did not. Furthermore, it was shown that compactification down to 4 dimensions (assuming N=1 SUSY) can lead to E_6 as an “effective” GUT group. Each family of SM particles now sits in its own **27**, Fig. 1. The generational problem may be solved because it is expected that any reasonable compactification scheme should generate the appropriate number of copies of the **27**. For instance in a Calabi-Yau compactification scheme [20],

$$E_8 \otimes E'_8 \longrightarrow SU(3) \otimes E_6 \otimes E'_8 ,$$

the number of generations is related to the topology of the compactified space. A further assertion that the matter fields remain supersymmetrically degenerate ensures proper management of any gauge hierarchical and fine tuning problems. It is assumed that the hidden sector, E'_8 , which couples to the matter fields of E_6 by gravitational interactions will provide a mechanism for lifting the degeneracy.

So the inspiration for using E_6 is that if it proves to be a possible GUT then it opens up the possibility of finding a TOE (**T**heory **O**f **E**verything). However, it should be pointed out that E_6 is not the only possible stop *en route* to the SM, but it is the most studied [4]. It is for this reason that the low energy phenomenology resulting from E_6 will be considered.

A. E_6 Phenomenology

1. An extra Z_E

In order to produce the SM gauge structure, E_6 must be broken. Also, to handle any hierarchical and fine tuning problems, SUSY must be preserved [20]. This restriction makes the task more difficult, using most naïve breaking schemes. The solution to the problem was found by using a Wilson-loop mechanism [20] over the non-simply-connected-compactified-string-manifold to factor out the various subgroups of E_6 . Fig. 2 shows some of the possible,

$\Phi_A = \Phi(A, \tilde{A})$ is the superfield, such that $A = R', Q, u_L^c, \dots$, and

$$\Phi_Q = \begin{pmatrix} \Phi_u \\ \Phi_d \end{pmatrix}_L, \quad \Phi_L = \begin{pmatrix} \Phi_{\nu_e} \\ \Phi_e \end{pmatrix}_L, \quad \Phi_{L'} = \begin{pmatrix} \Phi_{\nu'_e} \\ \Phi_{e'} \end{pmatrix}_L, \quad \Phi_{R'} = \begin{pmatrix} \Phi_{e'} \\ \Phi_{\nu'_e} \end{pmatrix}_L^c,$$

for the first generation of the **27**'s, and similarly for the other generations. The Yukawa couplings, λ_i 's, also carry generational which have been suppressed; the couplings are inter-generational as well as intra-generational. The superpotential, W , summarizes the entire possible spectrum of low energy physics which can occur within the context of an E_6 framework.

Notice that W was only required to be invariant under the SM gauge group. Further constraints from E_6 model building may cause some of the λ_i terms to disappear. Furthermore, not all of these terms can simultaneously exist without giving rise to $\Delta L \neq 0$ and $\Delta B \neq 0$ interactions; E_6 models say nothing about the assignments of baryon (B) and lepton (L) number until they are connected to SM representations. As a result various scenarios may occur,

- Leptoquarks: $B(q'_L) = \frac{1}{3}, L(q'_L) = 1 \implies \lambda_9 = \lambda_{10} = 0$
- Diquarks : $B(q'_L) = -\frac{2}{3}, L(q'_L) = 0 \implies \lambda_6 = \lambda_7 = \lambda_8 = 0$
- Quarks : $B(q'_L) = \frac{1}{3}, L(q'_L) = 0 \implies \lambda_6 = \lambda_7 = \lambda_8 = \lambda_9 = \lambda_{10} = 0$

where it has been assumed that $L(\nu_L^c) = -1$ (these scenarios assume that there exist only three copies of the **27**; more complicated ones can be constructed by adding extra copies). In this paper the least exotic of these models, *i.e.*, the ‘‘Quarks,’’ will be investigated. Furthermore, to avoid any fine tuning problems with the neutrino masses,

$$m_{\nu_{eL}^c} \ll m_e \iff \lambda_{11} \ll \lambda_3,$$

it will be assumed $\lambda_{11} = 0$.

In this model the masses of the particles are generated by letting the role of the Higgs fields be played by

$$\tilde{L}' = \begin{pmatrix} \tilde{\nu}'_{eL} \\ \tilde{e}'_L \end{pmatrix}, \quad \tilde{R}' = \begin{pmatrix} \tilde{e}^c_L \\ \tilde{\nu}^c_{eL} \end{pmatrix}, \quad \tilde{\nu}^c_{eL},$$

for each generation. It is possible to work in a basis where only the third generation of Higgses acquire a VEV; the remainder become “unHiggses” [4,5]. In this basis the Yukawa couplings,

$$\lambda_4^{ijk} \Phi_{R'_i} \Phi_{L'_j} \Phi_{\nu''_k} ,$$

where $i, j, k = 1, 2, 3$ are generational indices, takes on a much simpler form,

$$\lambda_4 \in \{ \lambda_4^{ijk} | \lambda_4^{i33} = \lambda_4^{3i3} = \lambda_4^{33i} = 0, \lambda_4^{333} = \lambda_4^{3jk} = \lambda_4^{j3k} = \lambda_4^{jk3} \neq 0 \text{ s.t. } i = 1, 2 \text{ \& } j, k = 1, 2, 3 \} .$$

This basis also eliminates the potential problem of flavour changing neutral currents at the tree level. It is also assumed that the λ_i 's are real and that the couplings to the unHiggses are very small. The former assumption helps to further simplify the model and reduce any effects it might have in the CP violation sector [4].

B. Heavy Lepton Production

E_6 models are very rich in their spectrum of possible low energy phenomenological predictions. If any new particles are found that fit within this framework then perhaps it will lead the way to a more unified theory of the fundamental forces of nature. However this is no small task, for a full theory would have to be able to actually predict the mass spectrum of the particles and the relationships between various couplings, and yet require very few parameters. Superstring inspired E_6 models are far from being able to complete this task. However, proof that E_6 is an effective GUT would be a good first step. But even this would not necessarily qualify superstrings to be the next step for it is not totally inconceivable that some other theory might give rise to E_6 as an effective GUT — *caveat emptor*.

A natural question to ask would be, “Where to look for E_6 phenomenology?” High energy hadron colliders, such as the TEVATRON at Fermilab (1.8 TeV c.o.m., $\mathcal{L} \sim 10^2 pb^{-1}/yr$, $p\bar{p}$) or the LHC (14 TeV c.o.m., $\mathcal{L} \sim 10^5 pb^{-1}/yr$, pp), offer possibilities of observing phenomena beyond the SM by looking for the production of heavy leptons through a mechanism known as gluon-gluon fusion [25,26], see Fig. 3. This is an interesting process because there are

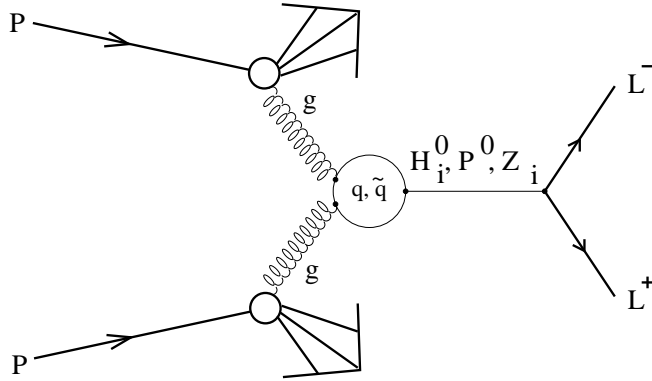


FIG. 3. Gluon-gluon fusion to two heavy leptons, $gg \rightarrow L^+L^-$. The loop contains quarks, q , which couple to vector bosons, $Z_{i=1,2}$, scalar-Higgses, $H_{i=1,2,3}^0$, and a pseudo-scalar-Higgs, P^0 , and squarks, \tilde{q} , which couple to scalar-Higgses.

enhancements in the cross-sections related to the heavy (s)fermions running around in the loop. The computation was done in the minimal supersymmetric standard model (MSSM) by Cieza Montalvo, *et al.*, [27] in which they predict $\mathcal{O}(10^5)$ *events/yr*. Therefore for E_6 is it expected that the production rate should in principle be higher since there are more particles running around in the loop.

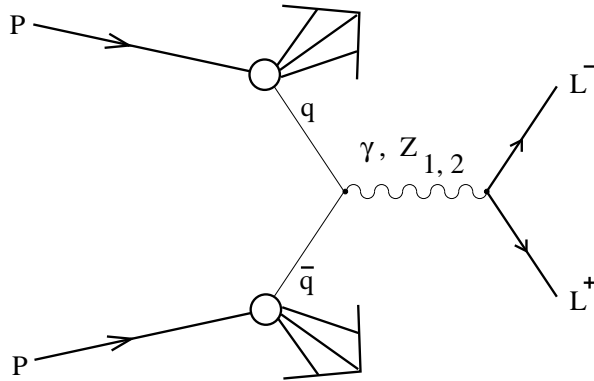


FIG. 4. Drell-Yan, direct, production to two heavy leptons, $q\bar{q} \rightarrow L^+L^-$.

The other contribution to L^+L^- production is the Drell-Yan mechanism, see Fig. 4. In general, this is expected to be small for L^+L^- invariant masses above the Z resonances

[25,26]. Indeed, for *MSSM* it is the least dominant effect. However, since E_6 has an extra vector boson, Z' , that is fairly massive, it is expected that Drell-Yan production will compete with gluon-gluon fusion below the Z' threshold.

These processes will be investigated in this paper.

III. A LOW ENERGY E_6 MODEL

In section I, a general overview of superstring inspired E_6 models was given. In addition, several comments were made about the type of model that would be presented. We shall now expand on these assumptions to determine their low energy consequences.

There are many ways of breaking E_6 down to SM energies. Invariably these breaking schemes lead to SM phenomenologies which contain extra gauge bosons. Here a rather simple model was chosen in which only an extra Z , the Z' , is produced [4,7,8]:

$$E_6 \longrightarrow SU(3)_c \otimes SU(2)_L \otimes U(1)_Y \otimes U(1)_{Y_E}$$

(*cf.* Fig. 2). In general the Z' can mix with the SM Z to produce the mixed states

$$Z_1 = \cos \phi Z + \sin \phi Z', \quad (2)$$

$$Z_2 = -\sin \phi Z + \cos \phi Z', \quad (3)$$

[*cf.* Eq. (46)].

Recall that in order to avoid potential problems with flavour-changing-neutral currents, at the tree level, a basis was chosen in which the third generation of primed-exotic-sleptons were assigned to play the role of the Higgses [4,5]:

$$\tilde{L}'_3 = \begin{pmatrix} \tilde{\nu}'_{\tau_L} \\ \tilde{\tau}'_L \end{pmatrix}, \quad \tilde{R}'_3 = \begin{pmatrix} \tilde{\tau}''_L{}^c \\ \tilde{\nu}''_{\tau_L}{}^c \end{pmatrix}, \quad \tilde{\nu}''_{\tau_L}{}^c, \quad (4)$$

(*i.e.*, $\tilde{R}'_3 \equiv \tilde{L}'_3{}^c$) or by redefining \tilde{L}'_3 , \tilde{R}'_3 and $\tilde{\nu}''_{\tau_L}{}^c$, in terms of the complex-isodoublet fields, Φ_1 and Φ_2 , and the complex-isoscalar field, Φ_3 , respectively, Eq. (4) becomes

$$\Phi_1 = \begin{pmatrix} \phi_1^0 \\ \phi_1^- \end{pmatrix}, \quad \Phi_2 = \begin{pmatrix} \phi_2^+ \\ \phi_2^0 \end{pmatrix}, \quad \Phi_3 = \phi_3^0. \quad (5)$$

This assignment was accomplished by setting

$$\left. \begin{aligned} \lambda_4^{i33} = \lambda_4^{3i3} = \lambda_4^{33i} = 0 & \quad i = 1, 2 \\ \lambda_4^{333} = \lambda_4^{3jk} = \lambda_4^{j3k} = \lambda_4^{jk3} \neq 0 & \quad j, k = 1, 2, 3 \end{aligned} \right\} \quad (6)$$

in the superpotential, Eq. (1), where the ijk 's are generation indices. Therefore in order to avoid lepton-number violation the lepton-numbers of all of the primed and double-primed exotic-leptons must be zero.

Further restrictions were placed on the superpotential by requiring that the baryon and lepton numbers of the exotic-quarks, q' , of the **27**'s (Fig. 1), are the same as those of their non-exotic SM counterparts [4]:

$$B(q'_L) = \frac{1}{3}, \quad L(q'_L) = 0 \quad \Rightarrow \quad \lambda_6 = \lambda_7 = \lambda_8 = \lambda_9 = \lambda_{10} = 0.$$

Also λ_{11} was set equal to zero in order to avoid any fine tuning problems with the $\nu_{L'}^c$ masses [4].

With all the aforementioned assumptions about the Yukawa couplings, the superpotential now simplifies to

$$\begin{aligned} W = & \lambda_1 i \Phi_Q^T \tau_2 \Phi_{R'} \Phi_{u_L^c} + \lambda_2 i \Phi_{L'}^T \tau_2 \Phi_Q \Phi_{d_L^c} + \lambda_3 i \Phi_{L'}^T \tau_2 \Phi_L \Phi_{e_L^c} \\ & + \lambda_4 i \Phi_{R'}^T \tau_2 \Phi_{L'} \Phi_{\nu_{e_L}^{\prime c}} + \lambda_5 \Phi_{d_L'} \Phi_{d_L^c} \Phi_{\nu_{e_L}^{\prime c}} \end{aligned} \quad (7)$$

where the λ 's were chosen to be real, plus similar terms for the other generations and their cross-terms. The $\Phi_A = \Phi(\psi_A, A)$ are the superfields which contain a two-component-spinor field, ψ_A , and a complex-scalar-singlet field, A . Table I summarizes the particle properties of this model.

The superpotential specifies all of the couplings between the particles of the **27**'s. According to appendix B of Haber and Kane [16], the Yukawa interactions are given by

$$\mathcal{L}_{\text{Yuk}} = -\frac{1}{2} \left[\left(\frac{\partial^2 W}{\partial A_i \partial A_j} \right) \Big|_{\psi'_A s=0} \psi_i \psi_j + \left(\frac{\partial^2 W}{\partial A_i \partial A_j} \right)^* \Big|_{\psi'_A s=0} \bar{\psi}_i \bar{\psi}_j \right] \quad (8)$$

TABLE I. Table of $SU(3)_c \otimes SU(2)_L \otimes U(1)_Y \otimes U(1)_{Y_E}$ particle properties.

	Q	L	u_L^c	d_L^c	e_L^c	ν_{eL}^c	d_L'	$d_L'^c$	L'	R'	$\nu_{eL}''^c$
c	3	1	$\bar{3}$	$\bar{3}$	1	1	3	$\bar{3}$	1	1	1
I_3	$\begin{pmatrix} 1/2 \\ -1/2 \end{pmatrix}$	$\begin{pmatrix} 1/2 \\ -1/2 \end{pmatrix}$	0	0	0	0	0	0	$\begin{pmatrix} 1/2 \\ -1/2 \end{pmatrix}$	$\begin{pmatrix} 1/2 \\ -1/2 \end{pmatrix}$	0
Y	1/3	-1	-4/3	2/3	2	0	-2/3	2/3	-1	1	0
Y_E	2/3	-1/3	2/3	-1/3	2/3	5/3	-4/3	-1/3	-1/3	-4/3	5/3
Q	$\begin{pmatrix} 2/3 \\ -1/3 \end{pmatrix}$	$\begin{pmatrix} 0 \\ -1 \end{pmatrix}$	-2/3	1/3	-1	0	-1/3	1/3	$\begin{pmatrix} 0 \\ -1 \end{pmatrix}$	$\begin{pmatrix} 1 \\ 0 \end{pmatrix}$	0
B	1/3	0	-1/3	-1/3	0	0	1/3	-1/3	0	0	0
L	0	1	0	0	-1	-1	0	0	0	0	0

and the scalar interactions are given by

$$V = V_F + V_D + V_{Soft}. \quad (9)$$

In Eq. (9), we have

$$V_F = F_i^* F_i, \quad (10)$$

$$V_D = \frac{1}{2} [D^a D^a + (D')^2], \quad (11)$$

with

$$F_i = \left. \left(\frac{\partial W}{\partial A_i} \right) \right|_{\psi'_A s=0}, \quad (12)$$

$$D^a = g A_i^* T_{ij}^a A_j, \quad (13)$$

$$D' = \frac{1}{2} g' Y_i A_i^* A_i, \quad (14)$$

where g represents an $SU(N)$ coupling constant with generators T^a , and g' represents a $U(1)$ coupling constant with hypercharge Y . V_{Soft} is a soft-SUSY-breaking term that was put in by hand in order to lift the supersymmetric-mass-degeneracy between m_{ψ_A} and m_A :

$$V_{Soft} = V_{\tilde{q}} + V_{\tilde{l}} + V_{H_{Soft}}, \quad (15)$$

with

$$V_{\tilde{q}} \supseteq \tilde{M}_Q^2 |\tilde{Q}|^2 + \tilde{M}_u^2 \tilde{u}_R^* \tilde{u}_R + \tilde{M}_d^2 \tilde{d}_R^* \tilde{d}_R + \tilde{M}_{d'_L}^2 \tilde{d}'_{L*} \tilde{d}'_L + \tilde{M}_{d'_R}^2 \tilde{d}'_{R*} \tilde{d}'_R + 2 \operatorname{Re} [\lambda_1 A_u i \tilde{Q}^T \tau_2 \Phi_2 \tilde{u}_R^* + \lambda_2 A_d i \Phi_1^T \tau_2 \tilde{Q} \tilde{d}_R^* + \lambda_5 A_{d'} \tilde{d}'_{R*} \tilde{d}'_L \Phi_3], \quad (16)$$

$$V_{\tilde{l}} \supseteq \tilde{M}_L^2 |\tilde{L}|^2 + \tilde{M}_e^2 \tilde{e}_R^* \tilde{e}_R + \tilde{M}_{\nu_e}^2 \tilde{\nu}_{eR}^* \tilde{\nu}_{eR} + 2 \lambda_3 A_e \operatorname{Re} [i \Phi_1^T \tau_2 \tilde{L} \tilde{e}_R^*], \quad (17)$$

$$V_{H_{soft}} = \mu_1^2 |\Phi_1|^2 + \mu_2^2 |\Phi_2|^2 + \mu_3^2 |\Phi_3|^2 - \frac{1}{\sqrt{2}} \lambda A (i \Phi_1^T \tau_2 \Phi_2 \Phi_3 + h.c.). \quad (18)$$

The coefficients \tilde{M}_A^2 , A_A , μ_i^2 , and A are the soft-SUSY-breaking parameters, and $\lambda \equiv \lambda_4^{333}$.

The Higgs potential can be extracted directly from Eq. (9) and is given by [4,8,9]

$$\begin{aligned} V_H &= V_{H_{soft}} + \lambda^2 (|\Phi_1|^2 |\Phi_2|^2 + |\Phi_1|^2 |\Phi_3|^2 + |\Phi_2|^2 |\Phi_3|^2) \\ &\quad + \frac{1}{8} (g^2 + g'^2) (|\Phi_1|^2 - |\Phi_2|^2)^2 + \frac{1}{72} g''^2 (|\Phi_1|^2 + 4|\Phi_2|^2 - 5|\Phi_3|^2)^2 \\ &\quad + (\frac{1}{2} g^2 - \lambda^2) |\Phi_1^\dagger \Phi_2|^2, \end{aligned} \quad (19)$$

where g , g' , and g'' are the $SU(2)_L$, $U(1)_Y$, and $U(1)_{Y_E}$ coupling constants, respectively.

The minimization condition [4]

$$\left. \frac{\partial V_H}{\partial \phi_i^0} \right|_{VEV's} = 0, \quad (20)$$

can be used to fix the μ_i^2 terms in $V_{H_{soft}}$ [Eq. (18)], where the vacuum expectation values, VEV 's, are given by

$$\langle \Psi \rangle = \begin{cases} \frac{\nu_i}{\sqrt{2}} & \text{if } \Psi = \phi_i^0 \\ 0 & \text{otherwise} \end{cases} \in \mathfrak{R}. \quad (21)$$

Therefore, we have

$$\begin{aligned} \mu_i^2 &= \frac{3}{72} g''^2 (v_1^2 + 4v_2^2 - 5v_3^2) Y_{E_i} + \frac{1}{8} (g^2 + g'^2) (\nu_1^2 - \nu_2^2) Y_i \\ &\quad - \sum_{j < k} \tilde{\varepsilon}_{ijk} \left[\frac{(v_j^2 + v_k^2)}{2} \lambda^2 - \frac{\nu_j \nu_k}{4\nu_i} \lambda A \right] \end{aligned} \quad (22)$$

where $\tilde{\varepsilon}_{ijk} = |\varepsilon_{ijk}|$. The kinetic terms for the scalar fields are given by [28]

$$\mathcal{L}_{K.E.} \supseteq |\mathcal{D}_\mu \Phi_i|^2 \equiv |(\partial_\mu - \frac{i}{2} G_\mu) \Phi_i|^2, \quad (23)$$

with (*cf.* [4])

$$G_\mu = (g\tau_3 \sin \theta_W + g'Y \cos \theta_W)A_\mu + (g\tau_3 \cos \theta_W - g'Y \sin \theta_W)Z_\mu \\ + \sqrt{2}g[\tau_+ W_\mu^- + \tau_- W_\mu^+] + g''Y_E Z'_\mu, \quad (24)$$

where $\tau_\pm = \frac{1}{2}(\tau_1 \pm i\tau_2)$, $\tau_i|\Phi_3\rangle \equiv 0$, and $g' \approx g''$ [4,6]. The τ_i 's are the Pauli matrices acting in isospin space.

The Φ_i fields have complex components, ϕ_i^a , which were chosen to be of the form [5,28] (*cf.* [29])

$$\phi_i^a = \frac{1}{\sqrt{2}}(\phi_{iR}^a + i\phi_{iI}^a), \quad (25)$$

where $\phi_{iR}^a/\sqrt{2}$ and $\phi_{iI}^a/\sqrt{2}$ are the real and imaginary parts, respectively. Therefore, the $\{\Phi_i\}$ fields have a total 10 degrees of freedom: four are “eaten” to give masses to the W^\pm , Z , and Z' bosons, and the remainder yield [4] two charged-Higgs bosons, H^\pm , one pseudo-scalar-Higgs boson, P^0 , and three scalar-Higgs bosons, $H_{i=1,2,3}^0$. The mass terms for the Higgs fields can be obtained from the second order terms of the expansion of $V_H(\phi_k)$ about its minimum [28],

$$V_H(\phi_k) \supseteq \frac{1}{2} \mathcal{M}_{ij}^2 (\phi_i - \langle \phi_i \rangle)(\phi_j - \langle \phi_j \rangle), \quad (26)$$

where

$$\mathcal{M}_{ij}^2 = \left. \frac{\partial^2 V_H}{\partial \phi_i \partial \phi_j} \right|_{VEV's} \quad (27)$$

is the Higgs-mass-mixing matrix. Therefore the mass terms for the Higgs fields are simply

$$\mathcal{L}_M \supseteq -(\phi_2^{+*} \phi_1^-) \mathcal{M}_{H^\pm}^2 \begin{pmatrix} \phi_2^+ \\ \phi_1^{-*} \end{pmatrix} - \frac{1}{2} (\phi_{2I}^0 \phi_{1I}^0 \phi_{3I}^0) \mathcal{M}_{P^0}^2 \begin{pmatrix} \phi_{2I}^0 \\ \phi_{1I}^0 \\ \phi_{3I}^0 \end{pmatrix} \\ - \frac{1}{2} (\phi_{1R}^0 - \nu_1 \phi_{2R}^0 - \nu_2 \phi_{3R}^0 - \nu_3) \mathcal{M}_{H_i^0}^2 \begin{pmatrix} \phi_{1R}^0 - \nu_1 \\ \phi_{2R}^0 - \nu_2 \\ \phi_{3R}^0 - \nu_3 \end{pmatrix}. \quad (28)$$

The mass-mixing matrices are

$$\mathcal{M}_{H^\pm}^2 = \frac{1}{2} \begin{pmatrix} (\frac{1}{2}g^2 - \lambda^2)\nu_1^2 + \lambda A \frac{\nu_{13}}{\nu_2} & (\frac{1}{2}g^2 - \lambda^2)\nu_{12} + \lambda A \nu_3 \\ (\frac{1}{2}g^2 - \lambda^2)\nu_{12} + \lambda A \nu_3 & (\frac{1}{2}g^2 - \lambda^2)\nu_2^2 + \lambda A \frac{\nu_{23}}{\nu_1} \end{pmatrix}, \quad (29)$$

$$\mathcal{M}_{P^0}^2 = \frac{\lambda A \nu_3}{2} \begin{pmatrix} \frac{\nu_1}{\nu_2} & 1 & \frac{\nu_1}{\nu_3} \\ 1 & \frac{\nu_2}{\nu_1} & \frac{\nu_2}{\nu_3} \\ \frac{\nu_1}{\nu_3} & \frac{\nu_2}{\nu_3} & \frac{\nu_1^2}{\nu_3^2} \end{pmatrix}, \quad (30)$$

$$\mathcal{M}_{H_i^0}^2 = \frac{1}{2} \begin{pmatrix} B_1 \nu_1^2 + \lambda A \frac{\nu_{23}}{\nu_1} & B_2 \nu_{12} - \lambda A \nu_3 & B_3 \nu_{13} - \lambda A \nu_2 \\ B_2 \nu_{21} - \lambda A \nu_3 & B_4 \nu_2^2 + \lambda A \frac{\nu_{13}}{\nu_2} & B_5 \nu_{23} - \lambda A \nu_1 \\ B_3 \nu_{31} - \lambda A \nu_2 & B_5 \nu_{32} - \lambda A \nu_1 & B_6 \nu_3^2 + \lambda A \frac{\nu_{12}}{\nu_3} \end{pmatrix} \quad (31)$$

where $\nu_{ij} = \nu_i \nu_j$. In Eq. (31)

$$\left. \begin{aligned} B_1 &= \frac{1}{2}(g^2 + g'^2) + \frac{1}{18}g''^2 & B_2 &= 2\lambda^2 + \frac{2}{9}g''^2 - \frac{1}{2}(g^2 + g'^2) & B_3 &= 2\lambda^2 - \frac{5}{18}g''^2 \\ B_4 &= \frac{1}{2}(g^2 + g'^2) + \frac{8}{9}g''^2 & B_5 &= 2\lambda^2 - \frac{10}{9}g''^2 \\ B_6 &= \frac{25}{18}g''^2 \end{aligned} \right\}. \quad (32)$$

The physical states are obtained by diagonalizing the terms in $\mathcal{L}_{\mathcal{M}}$. The eigenvectors for the charged and pseudo-scalar Higgs terms are respectively,

$$H^\pm = \cos \beta \phi_2^\pm + \sin \beta \phi_1^\pm, \quad (33)$$

$$G^\pm = -\sin \beta \phi_2^\pm + \cos \beta \phi_1^\pm, \quad (34)$$

and

$$P^0 = \sqrt{\frac{\lambda A \nu_3}{2m_{P^0}^2}} \left[\sqrt{\frac{\nu_1}{\nu_2}} \phi_{2I}^0 + \sqrt{\frac{\nu_2}{\nu_1}} \phi_{1I}^0 + \sqrt{\frac{\nu_{12}}{\nu_3^2}} \phi_{3I}^0 \right], \quad (35)$$

$$G_1^0 = \frac{\nu_2^2 \nu_3}{\sqrt{(\nu_2^2 + \nu_3^2)(\nu_{12}^2 + \nu^2 \nu_3^2)}} \left[\frac{\nu_3}{\nu_2} \phi_{2I}^0 - \frac{\nu_1}{\nu_3} \left(1 + \frac{\nu_3^2}{\nu_2^2} \right) \phi_{1I}^0 + \phi_{3I}^0 \right], \quad (36)$$

$$G_2^0 = \frac{\nu_3}{\sqrt{\nu_2^2 + \nu_3^2}} \left[-\frac{\nu_2}{\nu_3} \phi_{2I}^0 + \phi_{3I}^0 \right], \quad (37)$$

where $\phi_i^\pm = (\phi_i^\mp)^*$, $\nu^2 = \nu_1^2 + \nu_2^2$, and $\tan \beta \equiv \nu_2/\nu_1$. Here, the H^\pm are the charged-Higgs states with masses

$$m_{H^\pm}^2 = \frac{\lambda A \nu_3}{\sin(2\beta)} + \left(1 - 2 \frac{\lambda^2}{g^2}\right) m_W^2, \quad (38)$$

the P^0 is the pseudo-scalar-Higgs state with mass

$$m_{P^0}^2 = \frac{\lambda A \nu_3}{\sin(2\beta)} \left(1 + \frac{\nu^2}{4\nu_3^2} \sin^2(2\beta)\right), \quad (39)$$

and the G^\pm and $G_{1,2}^0$ are the Goldstone-boson states with zero mass. The scalar-Higgs term can be diagonalized analytically, however the result is, in general, not very enlightening. For our purposes it suffices to resort to numerical techniques. In the unitary gauge (U-gauge) the Goldstone modes vanish, *i.e.*, the G 's = 0, and the fields become physical. This allows the change of basis:

$$\phi_1^\pm = \sin \beta H^\pm, \quad (40)$$

$$\phi_2^\pm = \cos \beta H^\pm, \quad (41)$$

$$\phi_{1I}^0 = \kappa \nu_{23} P^0, \quad (42)$$

$$\phi_{2I}^0 = \kappa \nu_{13} P^0, \quad (43)$$

$$\phi_{3I}^0 = \kappa \nu_{12} P^0, \quad (44)$$

$$\phi_{iR}^0 = \nu_i + \sum_{j=1}^3 U_{ij} H_j^0, \quad (45)$$

where $\kappa = 1/\sqrt{\nu_1^2 \nu_2^2 + \nu^2 \nu_3^2}$. The U_{ij} are the elements of the inverse of the matrix that was used in the similarity transformation to diagonalized the scalar-Higgs-mass term. With these transformations at hand it is now a straightforward matter to get all of the masses and couplings for the various particles in this model.

The mass terms for the gauge fields can be found by transforming the kinetic terms for the Φ_i fields, Eq. (23), to the U-gauge basis, Eqs. (40)-(45), yielding:

$$\mathcal{L}_{K.E.}^{\Phi_i} \supseteq m_W^2 W_\mu^+ W^{-\mu} + \frac{1}{2} (Z \ Z')_\mu \mathcal{M}_{Z-Z'}^2 \begin{pmatrix} Z \\ Z' \end{pmatrix}^\mu. \quad (46)$$

As a consequence, the W mass is

$$m_W^2 = \frac{1}{4} g^2 \nu^2, \quad (47)$$

and the $Z - Z'$ -mass-mixing matrix is [4,6–8]

$$\mathcal{M}_{Z-Z'}^2 = \begin{pmatrix} m_Z^2 & \delta m^2 \\ \delta m^2 & m_{Z'}^2 \end{pmatrix}, \quad (48)$$

with matrix elements:

$$m_Z^2 = \frac{1}{4}(g^2 + g'^2) \nu^2, \quad (49)$$

$$m_{Z'}^2 = \frac{1}{36} g''^2 (\nu_1^2 + 16\nu_2^2 + 25\nu_3^2), \quad (50)$$

$$\delta m^2 = \frac{1}{12} \sqrt{g^2 + g'^2} g'' (4\nu_2^2 - \nu_1^2). \quad (51)$$

Diagonalization of $\mathcal{M}_{Z-Z'}^2$ yields the mass eigenstates given by Eqs. (2) and (3) with eigenvalues

$$m_{Z_1}^2 = m_Z^2 \cos^2 \phi + \delta m^2 \sin(2\phi) + m_{Z'}^2 \sin^2 \phi, \quad (52)$$

$$m_{Z_2}^2 = m_Z^2 \sin^2 \phi - \delta m^2 \sin(2\phi) + m_{Z'}^2 \cos^2 \phi, \quad (53)$$

and mixing angle

$$\tan(2\phi) = \frac{2\delta m^2}{m_Z^2 - m_{Z'}^2}. \quad (54)$$

Notice that in the large ν_3 limit, $\phi \rightarrow \pi/2$, and therefore $Z_1 \rightarrow Z$, and $Z_2 \rightarrow Z'$. In fact for the range of VEV 's that will be considered here, $m_{Z_1} < m_{Z_2}$. Therefore, Z_1 will be designated the role of the observed Z , at facilities such as LEP or SLC.

The mass terms for the fermions, and hence the Yukawa couplings, can be found by evaluating \mathcal{L}_{Yuk} , Eq. (8), in the U-gauge basis and then using Appendix A of Haber and Kane [16], to convert to four component spinor notation.¹ The result is

$$\mathcal{L}_{Yuk} \supseteq -\frac{1}{\sqrt{2}} \left\{ \lambda_1 \nu_2 \bar{u}u + \lambda_2 \nu_1 \bar{d}d + \lambda_3 \nu_1 \bar{e}e + \lambda_4 \nu_3 \bar{e}'e' + \lambda_5 \nu_3 \bar{d}'d' \right\}. \quad (55)$$

Therefore, the Yukawa couplings for the first generation are given by:

¹*cf.* Eq. (A28). For a more explicit example see section 4.2 of Gunion and Haber [29]

$$\lambda_1 = \frac{g m_u}{\sqrt{2} m_W \sin \beta}, \quad (56)$$

$$\lambda_2 = \frac{g m_d}{\sqrt{2} m_W \cos \beta}, \quad (57)$$

$$\lambda_3 = \frac{g m_e}{\sqrt{2} m_W \cos \beta}, \quad (58)$$

$$\lambda_4 = \frac{\sqrt{2}}{\nu_3} m_{e'}, \quad (59)$$

$$\lambda_5 = \frac{\sqrt{2}}{\nu_3} m_{d'}, \quad (60)$$

and similarly for the other generations.

The sfermion masses are obtained by evaluating the scalar-interaction potential, V [Eq. (9)], and then transforming it to the U-gauge basis:

$$\mathcal{L}_{\mathcal{M}} \supseteq -V \supseteq -(\tilde{f}_L^* \tilde{f}_R^*) \mathcal{M}_{\tilde{f}}^2 \begin{pmatrix} \tilde{f}_L \\ \tilde{f}_R \end{pmatrix}, \quad (61)$$

with

$$\mathcal{M}_{\tilde{f}}^2 = \begin{pmatrix} M_{LL}^2 & M_{LR}^2 \\ M_{LR}^2 & M_{RR}^2 \end{pmatrix}, \quad (62)$$

being the sfermion-mass-mixing matrix. The mass-mixing matrix elements are given by:

$$M_{LL}^{(\tilde{u})^2} = \tilde{M}_Q^2 + m_u^2 + \frac{1}{6} (3 - 4x_W) m_Z^2 \cos(2\beta) - \frac{1}{36} g''^2 (\nu_1^2 + 4\nu_2^2 - 5\nu_3^2), \quad (63)$$

$$M_{RR}^{(\tilde{u})^2} = \tilde{M}_u^2 + m_u^2 + \frac{2}{3} x_W m_Z^2 \cos(2\beta) - \frac{1}{36} g''^2 (\nu_1^2 + 4\nu_2^2 - 5\nu_3^2), \quad (64)$$

$$M_{LR}^{(\tilde{u})^2} = m_u (A_u - m_{e'} \cot \beta), \quad (65)$$

for the $\tilde{u}_{L,R}$ squarks;

$$M_{LL}^{(\tilde{d})^2} = \tilde{M}_Q^2 + m_d^2 - \frac{1}{6} (3 - 2x_W) m_Z^2 \cos(2\beta) - \frac{1}{36} g''^2 (\nu_1^2 + 4\nu_2^2 - 5\nu_3^2), \quad (66)$$

$$M_{RR}^{(\tilde{d})^2} = \tilde{M}_d^2 + m_d^2 - \frac{1}{3} x_W m_Z^2 \cos(2\beta) + \frac{1}{72} g''^2 (\nu_1^2 + 4\nu_2^2 - 5\nu_3^2), \quad (67)$$

$$M_{LR}^{(\tilde{d})^2} = m_d (A_d - m_{e'} \tan \beta), \quad (68)$$

for the $\tilde{d}_{L,R}$ squarks;

$$M_{LL}^{(\tilde{d}')^2} = \tilde{M}_{d'_L}^2 + m_{d'}^2 + \frac{1}{6} x_W m_Z^2 \cos(2\beta) + \frac{1}{18} g'^2 (\nu_1^2 + 4\nu_2^2 - 5\nu_3^2), \quad (69)$$

$$M_{RR}^{(\tilde{d}')^2} = \tilde{M}_{d'_R}^2 + m_{d'}^2 - \frac{1}{3} x_W m_Z^2 \cos(2\beta) + \frac{1}{72} g'^2 (\nu_1^2 + 4\nu_2^2 - 5\nu_3^2), \quad (70)$$

$$M_{LR}^{(\tilde{d}')^2} = m_{d'} (A_{d'} - m_{e'} \frac{\nu_{12}}{\nu_3^2}), \quad (71)$$

for the $\tilde{d}'_{L,R}$ squarks;

$$M_{LL}^{(\tilde{e})^2} = \tilde{M}_L^2 + m_e^2 - \frac{1}{2} (1 - 2x_W) m_Z^2 \cos(2\beta) + \frac{1}{72} g'^2 (\nu_1^2 + 4\nu_2^2 - 5\nu_3^2), \quad (72)$$

$$M_{RR}^{(\tilde{e})^2} = \tilde{M}_e^2 + m_e^2 - x_W m_Z^2 \cos(2\beta) - \frac{1}{36} g'^2 (\nu_1^2 + 4\nu_2^2 - 5\nu_3^2), \quad (73)$$

$$M_{LR}^{(\tilde{e})^2} = m_e (A_e - m_{e'} \tan \beta), \quad (74)$$

for the $\tilde{e}_{L,R}$ sleptons;

$$M_{LL}^{(\tilde{\nu}_e)^2} = \tilde{M}_L^2 + m_{\nu_e}^2 + \frac{1}{2} m_Z^2 \cos(2\beta) + \frac{1}{72} g'^2 (\nu_1^2 + 4\nu_2^2 - 5\nu_3^2), \quad (75)$$

$$M_{RR}^{(\tilde{\nu}_e)^2} = \tilde{M}_{\nu_e}^2 - \frac{5}{72} g'^2 (\nu_1^2 + 4\nu_2^2 - 5\nu_3^2), \quad (76)$$

$$M_{LR}^{(\tilde{\nu}_e)^2} = 0, \quad (77)$$

for the $\tilde{\nu}_{L,R}$ sleptons, and similarly for the other generations. The mass eigenstates are given by

$$\begin{pmatrix} \tilde{f}_1 \\ \tilde{f}_2 \end{pmatrix} = \begin{pmatrix} \cos \theta_{\tilde{f}} & \sin \theta_{\tilde{f}} \\ -\sin \theta_{\tilde{f}} & \cos \theta_{\tilde{f}} \end{pmatrix} \begin{pmatrix} \tilde{f}_L \\ \tilde{f}_R \end{pmatrix} \quad (78)$$

with mass eigenvalues

$$m_{f_1}^2 = M_{LL}^2 \cos^2 \theta_{\tilde{f}} + M_{LR}^2 \sin(2\theta_{\tilde{f}}) + M_{RR}^2 \sin^2 \theta_{\tilde{f}}, \quad (79)$$

$$m_{f_2}^2 = M_{LL}^2 \sin^2 \theta_{\tilde{f}} - M_{LR}^2 \sin(2\theta_{\tilde{f}}) + M_{RR}^2 \cos^2 \theta_{\tilde{f}}, \quad (80)$$

and mixing angle

$$\tan(2\theta_{\tilde{f}}) = \frac{M_{LR}^2}{M_{LL}^2 - M_{RR}^2}. \quad (81)$$

Notice that for fairly large ν_3

$$\tan(2\theta_{\tilde{f}}) \sim \mathcal{O}\left(\frac{m_f A_f}{\nu_3^2}\right), \quad (82)$$

where the soft terms have been assumed to be large and degenerate. Therefore, in general, the mixing is only expected to affect the sfermions that have fairly heavy fermion partners.

The supersymmetric partner, or spartner, degrees of freedom for the neutral-Higgs fields (neutral-Higgsinos), ν'_{τ_L} , $\nu'^c_{\tau_L}$ and $\nu''^c_{\tau_L}$, along with the spartner degrees of freedom for the neutral gauge fields (neutral-gauginos), $\tilde{\gamma}$, \tilde{Z} , and \tilde{Z}' , mix to form a (6×6) neutralino, $\tilde{\chi}^0$, mass-mixing matrix.² Similarly the charged-Higgsinos, τ'_L and τ'^c_L , and the charged-gauginos, \tilde{W}^\pm , form a (2×2) chargino, $\tilde{\chi}^\pm$, mass-mixing matrix.³ By virtue of supersymmetry the neutralino and chargino mass-mixing matrices contain the same Yukawa and gauge couplings as their spartners, modulo soft terms.

The real and imaginary parts of the sfermion fields, $\tilde{\nu}'_{e_L}$, $\tilde{\nu}^c_{e_L}$, $\tilde{\nu}''^c_{e_L}$, $\tilde{\nu}'_{\mu_L}$, $\tilde{\nu}^c_{\mu_L}$, and $\tilde{\nu}''^c_{\mu_L}$, yield two separate (6×6) -mass-mixing matrices for the neutral-unHiggses [*cf.* Eq. (28) for ϕ_{iR}^0 and ϕ_{iI}^0], which contain the Yukawa couplings given in Eq. (6). In general, these mass-mixing matrices are expected to lead to very massive unHiggs states [5].

The spartner degrees of freedom for the neutral-unHiggses, ν'_{e_L} , $\nu'^c_{e_L}$, $\nu''^c_{e_L}$, ν'_{μ_L} , $\nu'^c_{\mu_L}$, and $\nu''^c_{\mu_L}$, form a (6×6) -mass-mixing matrix for the neutral-unHiggsinos. Therefore, the neutral-unHiggsino mass-mixing matrix contains the same Yukawa couplings as their neutral-unHiggs partners.

The sfermion fields \tilde{e}'_L , \tilde{e}^c_L , $\tilde{\mu}'_L$, and $\tilde{\mu}^c_L$, yield two separate (2×2) -mass-mixing matrices for the charged-unHiggses [*cf.* Eq. (28) for ϕ_i^\pm]. These matrices have a large number of unknown parameters and quite naturally acquire a very large mass [*cf.* [5]].

Finally, the spartner degrees of freedom for the charged-unHiggses give diagonalized mass eigenstates [see Eq. (55)] which correspond to the charged heavy leptons.

²A detailed study of the $\tilde{\chi}^0$ mass spectrum can be found in [30].

³The full form of these mass matrices can be found in Ellis, *et al.*, [5] and the details of how to obtain them can be found in appendix B of Haber and Kane [16].

IV. L^+L^- PRODUCTION IN E_6

A. Gluon-Gluon Fusion

Fig. 5 shows the Feynman diagrams used for computing the parton level gluon-gluon fusion to heavy leptons matrix elements. It was found that the E_6 matrix element compu-

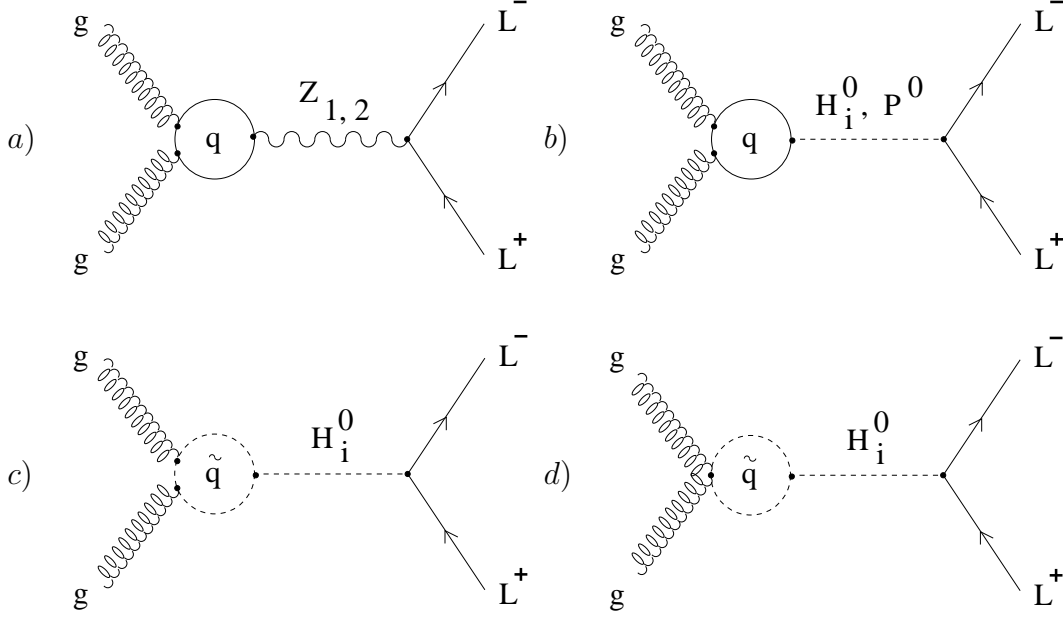


FIG. 5. Feynman diagrams for gluon-gluon fusion to charged heavy leptons.

tations are very similar to the corresponding $MSSM$ calculation by Cieza Montalvo, *et al.*, [27] (*cf.* [31]) and can, with some care, be extracted from their paper. The matrix elements are as follows:

1. For the $Z_{1,2}$ exchange diagram shown in Fig. 5(a)

$$\hat{\sigma}_{L^\pm}^{qZ_{1,2}} = \frac{\alpha^2 \alpha_s^2}{128\pi x_W^2} \frac{m_L^2}{m_W^4} \beta_L \left| \sum_{i=1}^2 [\tilde{C}_L^{L^\pm Z_i} - \tilde{C}_R^{L^\pm Z_i}] \xi^{Z_i}(\hat{s}) \sum_q [\tilde{C}_L^{qZ_i} - \tilde{C}_R^{qZ_i}] (1 + 2\lambda_q I_q) \right|^2 \quad (83)$$

where the left-right Fermion, f , couplings are given by

$$\begin{pmatrix} \tilde{C}_{L,R}^{fZ_1} \\ \tilde{C}_{L,R}^{fZ_2} \end{pmatrix} = \begin{pmatrix} \cos \phi & \sin \phi \\ -\sin \phi & \cos \phi \end{pmatrix} \begin{pmatrix} C_{L,R}^{fZ} \\ C_{L,R}^{fZ'} \end{pmatrix}, \quad (84)$$

such that

$$C_{L,R}^{fZ} = T_{3_{L,R}} - e_f x_W, \quad (85)$$

$$C_{L,R}^{fZ'} = \frac{1}{2} \left(\frac{g''}{g} \right) y'_{f_{L,R}} \sqrt{1 - x_W}, \quad (86)$$

where $T_{3_R} = -T_{3_L}^c$ is the isospin, $y'_{f_R} = -y'_{f_L^c}$ is the Y_E -hypercharge, and e_f is the electric charge.

2. For the $H_{1,2,3}^0$ and P^0 exchange diagrams shown in Fig. 5(b)

$$\hat{\sigma}_{L^\pm}^{qH_i^0 s} = \frac{\alpha^2 \alpha_s^2}{512 \pi x_W^2} \frac{m_L^2}{m_W^4} \beta_L^3 \left| \sum_{i=1}^3 K^{L^\pm H_i^0} \zeta^{H_i^0}(\hat{s}) \sum_q K^{qH_i^0} m_q^2 [2 + (4\lambda_q - 1)I_q] \right|^2, \quad (87)$$

$$\hat{\sigma}_{L^\pm}^{qP^0} = \frac{\alpha^2 \alpha_s^2}{512 \pi x_W^2} \frac{m_L^2}{m_W^4} \beta_L (K^{L^\pm P^0})^2 |\zeta^{P^0}(\hat{s})|^2 \left| \sum_q K^{qP^0} m_q^2 I_q \right|^2, \quad (88)$$

where the couplings $K^{fH_i^0}$ and K^{fP^0} are given by Eqs. (A29)-(A38).

3. For the $H_{1,2,3}^0$ exchange diagrams shown in Figs. 5(c) and 5(d)

$$\hat{\sigma}_{L^\pm}^{\tilde{q}H_i^0 s} = \frac{\alpha^2 \alpha_s^2 m_L \beta_L}{512 \pi x_W^2 (1 - x_W)^2} \left| \sum_{i=1}^3 K^{L^\pm H_i^0} \zeta^{H_i^0}(\hat{s}) \sum_{\tilde{q}} \sum_{k=1}^2 \tilde{K}_k^{\tilde{q}H_i^0} (1 + 2\lambda_{\tilde{q}_k} I_{\tilde{q}_k}) \right|^2, \quad (89)$$

where the sfermion mass eigenstates, $\tilde{f}_{1,2}$, couplings to the H_i^0 are given by

$$\tilde{K}_1^{\tilde{f}H_i^0} = K_{LL}^{\tilde{f}H_i^0} \cos^2 \theta_{\tilde{f}} + K_{LR}^{\tilde{f}H_i^0} \sin 2\theta_{\tilde{f}} + K_{RR}^{\tilde{f}H_i^0} \sin^2 \theta_{\tilde{f}}, \quad (90)$$

$$\tilde{K}_2^{\tilde{f}H_i^0} = K_{LL}^{\tilde{f}H_i^0} \sin^2 \theta_{\tilde{f}} - K_{LR}^{\tilde{f}H_i^0} \sin 2\theta_{\tilde{f}} + K_{RR}^{\tilde{f}H_i^0} \cos^2 \theta_{\tilde{f}}, \quad (91)$$

where $K_{AB}^{\tilde{f}H_i^0}$ ($A, B = L, R$) are the corresponding couplings for the sfermion helicity states, $\tilde{f}_{L,R}$, with mixing angle $\theta_{\tilde{f}}$. The $K_{AB}^{\tilde{f}H_i^0}$ couplings are given by Eqs. (A39)-(A54).

4. For the $q(Z_{1,2}-P^0)$ interference terms, *via* Figs. 5(a) and 5(b),

$$\begin{aligned} \hat{\sigma}_{L^\pm}^{\tilde{q}(Z_i'-P^0)} &= \frac{-\alpha^2 \alpha_s^2}{128 \pi x_W^2} \frac{m_L^2}{m_W^4} \beta_L K^{L^\pm P^0} \operatorname{Re} \left\{ \zeta^{P^0}(\hat{s}) \sum_{i=1}^2 \xi^{Z_i}(\hat{s})^* [\tilde{C}_L^{L^\pm Z_i} - \tilde{C}_R^{L^\pm Z_i}] \right. \\ &\quad \left. \times \sum_q K^{qP^0} m_q^2 I_q \sum_{q'} [\tilde{C}_L^{q' Z_i} - \tilde{C}_R^{q' Z_i}] (1 + 2\lambda_{q'} I_{q'}^*) \right\}. \end{aligned} \quad (92)$$

5. For the $(\tilde{q} - q)H_{1,2,3}^0$ interference terms, *via* Figs. 5(b)-5(d),

$$\begin{aligned}\hat{\sigma}_{L^\pm}^{(\tilde{q}-q)\tilde{H}_i^0's} &= \frac{-\alpha^2\alpha_s^2}{256\pi x_W^2(1-x_W)^2} \left(\frac{m_L}{m_Z}\right)^2 \beta_L^3 \operatorname{Re} \left\{ \sum_{i=1}^3 K^{L\pm H_i^0} \zeta^{H_i^0}(\hat{s}) \right. \\ &\quad \times \sum_q K^{qH_i^0} m_q^2 [2 + (4\lambda_q - 1)I_q] \sum_{j=1}^3 K^{L\pm H_j^0} \zeta^{H_j^0}(\hat{s})^* \\ &\quad \left. \times \sum_{\tilde{q}} \sum_{k=1}^2 \tilde{K}_k^{\tilde{q}H_j^0} (1 + 2\lambda_{\tilde{q}} I_{\tilde{q}}^*) \right\}.\end{aligned}\quad (93)$$

In the aforementioned list of cross-section equations,

$$\lambda_p = \frac{m_p^2}{\hat{s}}, \quad (94)$$

$$\begin{aligned}I_p &\equiv I_p(\lambda_p) = \int_0^1 \frac{dx}{x} \ln \left[1 - \frac{(1-x)x}{\lambda_p} \right] \\ &= \begin{cases} -2 \left[\sin^{-1} \left(\frac{1}{2\sqrt{\lambda_p}} \right) \right]^2 & \text{if } \lambda_p > \frac{1}{4} \\ \frac{1}{2} \ln^2 \left(\frac{r_+}{r_-} \right) - \frac{\pi^2}{2} + i\pi \ln \left(\frac{r_+}{r_-} \right) & \text{if } \lambda_p < \frac{1}{4} \end{cases},\end{aligned}\quad (95)$$

with $r_\pm = 1 \pm \sqrt{1 - 4\lambda_p}$ such that $p \in \{f, \tilde{f}\}$,

$$\xi^{Z_i}(\hat{s}) = \frac{\hat{s} - m_{Z_i}^2}{\hat{s} - m_{Z_i}^2 + i m_{Z_i} \Gamma_{Z_i}}, \quad (96)$$

$$\zeta^{H_i^0, P^0}(\hat{s}) = \frac{1}{\hat{s} - m_{H_i^0, P^0}^2 + i m_{H_i^0, P^0} \Gamma_{H_i^0, P^0}}, \quad (97)$$

where the $\Gamma_{V,\phi}$'s computations are summarized in § A 2, and

$$\beta_L = \sqrt{1 - \frac{4m_L^2}{\hat{s}}}. \quad (98)$$

The details of the various components that have gone into this computation can be found in appendix A. Before the parton level cross-section can be used to compute the heavy lepton production rates some assumptions about the parameters and masses in the model must be made.

The first thing that has to be constrained are the *VEV*'s. It is reasonable to assume that $v_1/v_2 \lesssim 1$, since $m_b \ll m_t$, for any reasonable range of Yukawa couplings [7,9]. Now the ratios v_1/v_2 and v_3/v_2 can be constrained by looking at how the variation in the Z_1 (*i.e.*, the “ Z ”) mass affects \bar{x}_W ($\equiv \sin^2 \bar{\theta}_W$) such that [7]

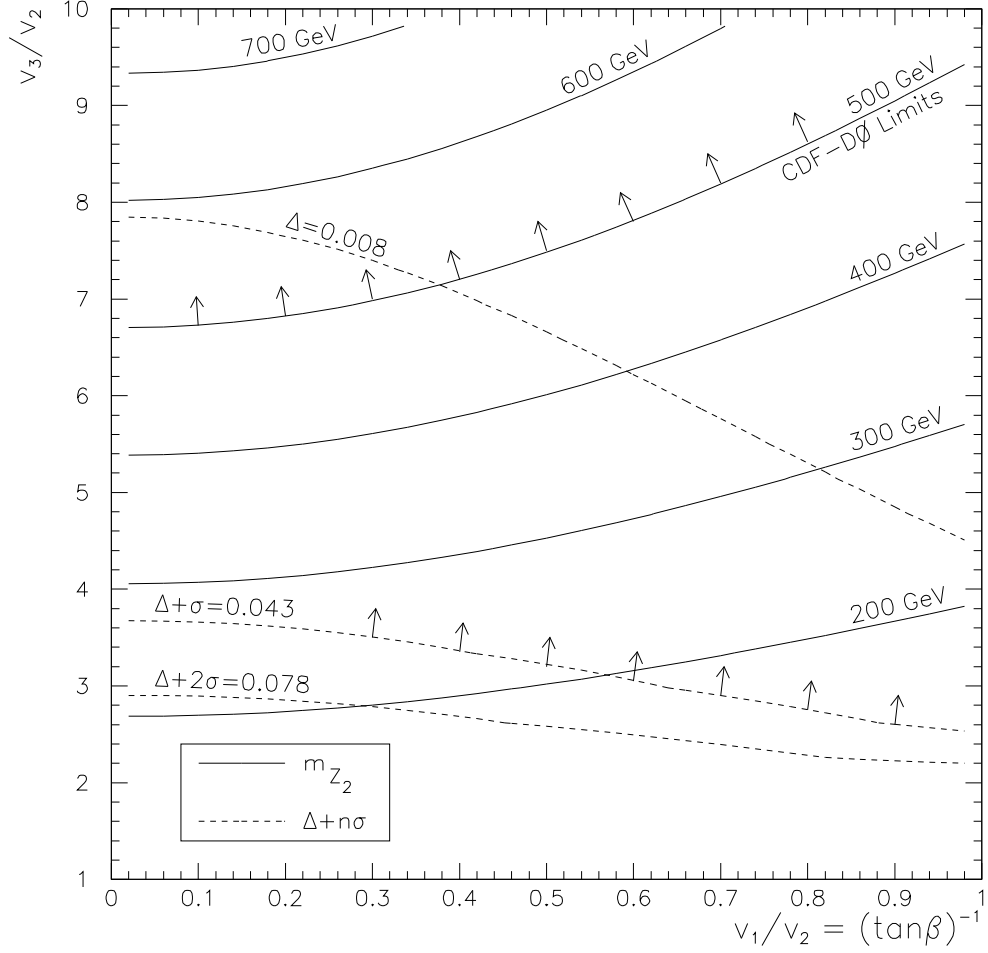


FIG. 6. Plot of m_{Z_2} and Δ contour lines as a function of v_3/v_2 and v_1/v_2 . The Δ contour lines are shown at the 0σ , 1σ , and 2σ levels. The arrows point to toward the allowed regions on the plot (*cf.* [7]). The $m_{Z_2} = 500 \text{ GeV}$ line shows the *CDF* and *D ϕ* constraints, assuming standard couplings [32].

$$\sin^2 \bar{\theta}_W \equiv 1 - \frac{m_W^2}{m_{Z_1}^2} < \sin^2 \theta_W \equiv \frac{g'^2}{g^2 + g'^2} \Big|_{\mu=m_W}. \quad (99)$$

$x_W(m_W)$ can be found by evolving $x_W(m_Z) \approx 0.2319 \pm 0.0005$ [33] down to m_W [25], which gives $x_W(m_W) \approx 0.233 \pm 0.035$, with $\alpha^{-1}(m_Z) \approx 127.9 \pm 0.1$ [33], $m_Z \approx (91.187 \pm 0.007) \text{ GeV}$ [33], and $m_W \approx (80.23 \pm 0.18) \text{ GeV}$ [32]. Therefore given $\bar{x}_W \approx 0.2247 \pm 0.0019$ [33] yields

$$\Delta \equiv x_W - \bar{x}_W \approx 0.008 \pm 0.035. \quad (100)$$

Fig. 6 shows the Δ contour line as a function of v_3/v_2 and v_1/v_2 , along with its 1σ and 2σ level contour lines. Also shown are the m_{Z_2} contour lines. Taking a 1σ level constraint implies $v_3/v_2 \gtrsim \mathcal{O}(3.5)$ (*cf.* [4,7]) and $m_{Z_2} \gtrsim \mathcal{O}(200) \text{ GeV}$. Unfortunately these constraints are not that tight due to the large uncertainty in $\alpha(m_Z)$. A stronger constraint can be found by using the CDF and $D\emptyset$ limits on the m_{Z_2} mass [32], assuming SM-like couplings, Fig. 6. This constraint is fairly reasonable since Y_E 's $\sim \mathcal{O}(Y)$'s (*cf.* table I). With these constraints $v_3/v_2 \gtrsim \mathcal{O}(7.5)$ and $m_{Z_2} \gtrsim \mathcal{O}(500) \text{ GeV}$.

Figs. 7 through 9 show H_1^0 mass contour plots as function of m_{P_0} and m_{H^\pm} for $(v_1/v_2, v_3/v_2) = (0.02, 6.7)$, $(v_1/v_2, v_3/v_2) = (0.5, 7.7)$, and $(v_1/v_2, v_3/v_2) = (0.9, 9.1)$, respectively, such that m_{Z_2} lies roughly around the CDF and $D\emptyset$ limits. These figures are a fairly good representation of the behavior of the $m_{H_1^0}$ contour lines as a function of v_1/v_2 . For fixed v_1/v_2 , the contour lines change very little (*i.e.*, $\lesssim \mathcal{O}(5)\%$) for $\mathcal{O}(10) \gtrsim v_3/v_2 \gtrsim \mathcal{O}(4.5)$. This region corresponds to the $(v_1/v_2, v_3/v_2)$ parameter space for $m_{Z_2} \gtrsim \mathcal{O}(300) \text{ GeV}$ depicted in Fig. 6. Further examination of the other scalar-Higgses shows $m_{H_3^0}$ is fairly insensitive to variations in m_{P_0} and m_{H^\pm} for fixed m_{Z_2} and is slightly sensitive to variations in v_3/v_2 , whereas the behaviour of $m_{H_2^0}$ appears to be quite sensitive to any variation. Fortunately for the range of VEV's considered here (*i.e.*, large v_3), the only contributions to the parton level cross-sections turn out to be the diagrams which contain the Z_i and H_3^0 propagators;

the other terms are, in general, suppressed by several orders of magnitude.⁴ Therefore the heavy lepton production cross-section is insensitive to variations in m_{P^0} and m_{H^\pm} . Here the P^0 mass will be set to 200 GeV . The corresponding H^\pm mass was chosen to be 215 GeV for Fig. 7 and 212 GeV for Figs. 8 and 9, which lies within the allowed regions on the m_{H^0} contour plots. Based on the very limited experimental constraints that do exist for supersymmetric models [33] these appear to be very conservative choices. They also lead to fairly reasonable values for the H_i^0 masses.

The next parameters that need to be fixed are the soft terms. Exactly how these terms should behave at low energy is not clear. At the moment, their behaviour is very model dependent and unless supersymmetric particles are found this situation will most likely remain so. Here the soft terms will be treated parametrically as function of a single parameter m_S . In particular the soft terms will be assumed to be degenerate, $\tilde{M}_f \approx A_f \approx m_S$, with the exception of the λ and A terms which were fixed by selecting the m_{P^0} and m_{H^\pm} masses. The selection of the soft terms in this way, including λ and A for $m_{P^0, H^\pm} \lesssim \mathcal{O}(1)\text{ TeV}$, typify the generic outcome, for the sfermion masses, of most SUSY-breaking models, *cf.* [6,9]. In these models $\mathcal{O}(0.2)\text{ TeV} \lesssim m_S \lesssim \mathcal{O}(10)\text{ TeV}$. How low m_S can be pushed down depends upon the choice of VEV's (v_3 in particular, since it is relatively large). For the VEV's used here it was found $m_S \gtrsim \mathcal{O}(400 - 450)\text{ GeV}$. In general the sfermions with light spartners have masses $\gtrsim \mathcal{O}(m_S)$, which are roughly degenerate (within $\mathcal{O}(50)\text{ GeV}$) with their mass-eigenstate partners. The stops, $\tilde{t}'_{1,2}$, and the exotic squarks, $\tilde{q}'_{1,2}$, have splittings $\gtrsim \mathcal{O}(\frac{1}{2}m_{t,q'})$, for fermion masses $\mathcal{O}(200) \lesssim m_{t,q'} \lesssim \mathcal{O}(600)\text{ GeV}$, for low values of m_S . As m_S approaches $\mathcal{O}(1)\text{ TeV}$ all of the sfermion mass become degenerate and $\approx \mathcal{O}(m_S)$.

⁴in the large v_3 limit the couplings $P^0 L^+ L^- \rightarrow 0$, *via* Eqs. (A18) and (A38), and $H_i^0 L^+ L^- \rightarrow -(m_L/v_3) \delta_{3i}$, *via* Eqs. (A17) and (A33), and Eq. (4.12) of Hewett and Rizzo [4] for the U_{3i} 's in this limit, to $\mathcal{O}(1/v_3)$.

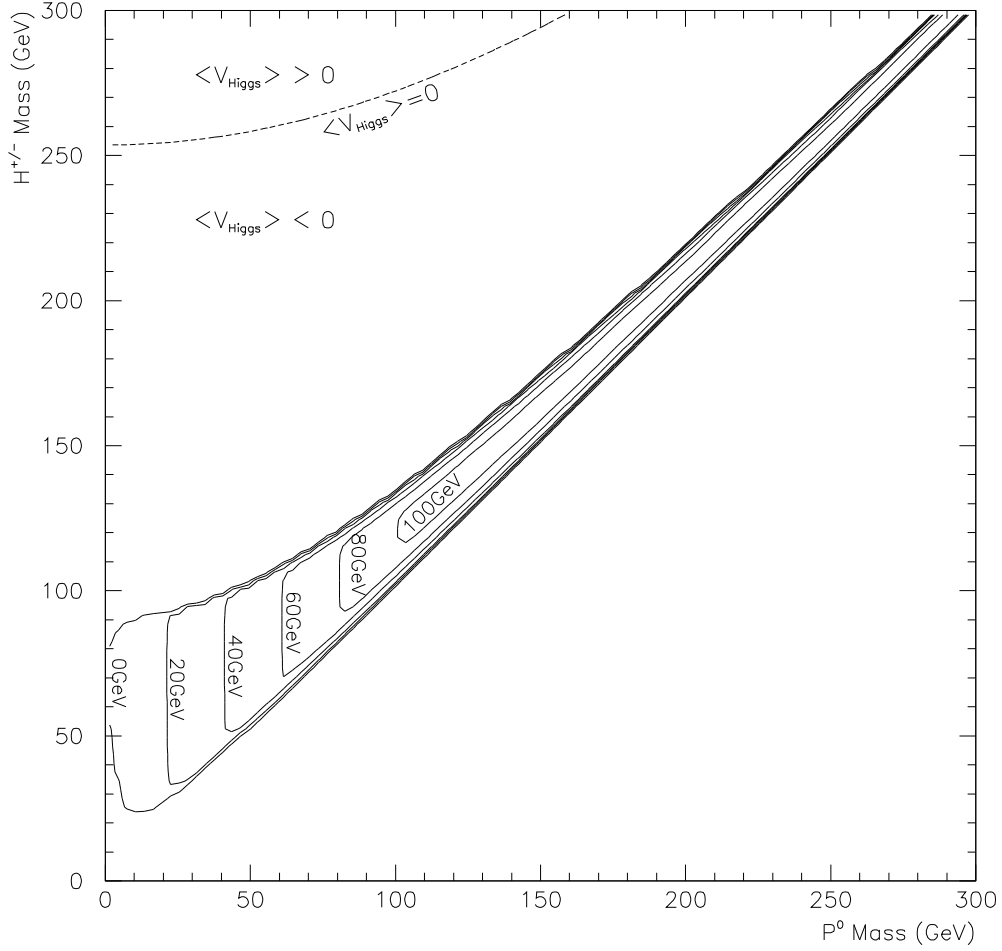


FIG. 7. A plot of the H_1^0 mass contour lines as a function of m_{P^0} and m_{H^\pm} , for $v_1/v_2 = 0.02$ and $v_3/v_2 = 6.7$ ($m_{Z_2} \approx 496 \text{ GeV}$). The dashed curve in the upper left-hand corner is a plot of the zero of the Higgs potential above which it becomes positive.

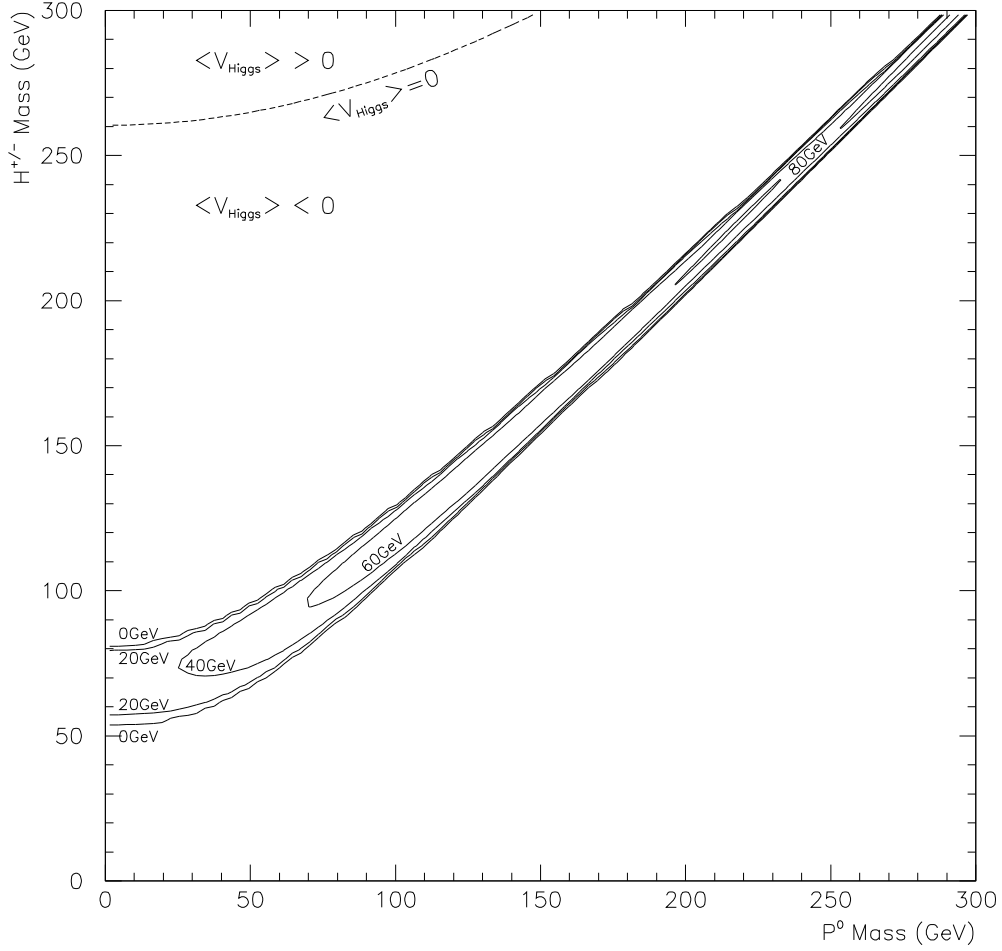


FIG. 8. A plot of the H_1^0 mass contour lines as a function of m_{P^0} and m_{H^\pm} , for $v_1/v_2 = 0.5$ and $v_3/v_2 = 7.7$ ($m_{Z_2} \approx 509 \text{ GeV}$). The dashed curve in the upper left-hand corner is a plot of the zero of the Higgs potential above which it becomes positive.

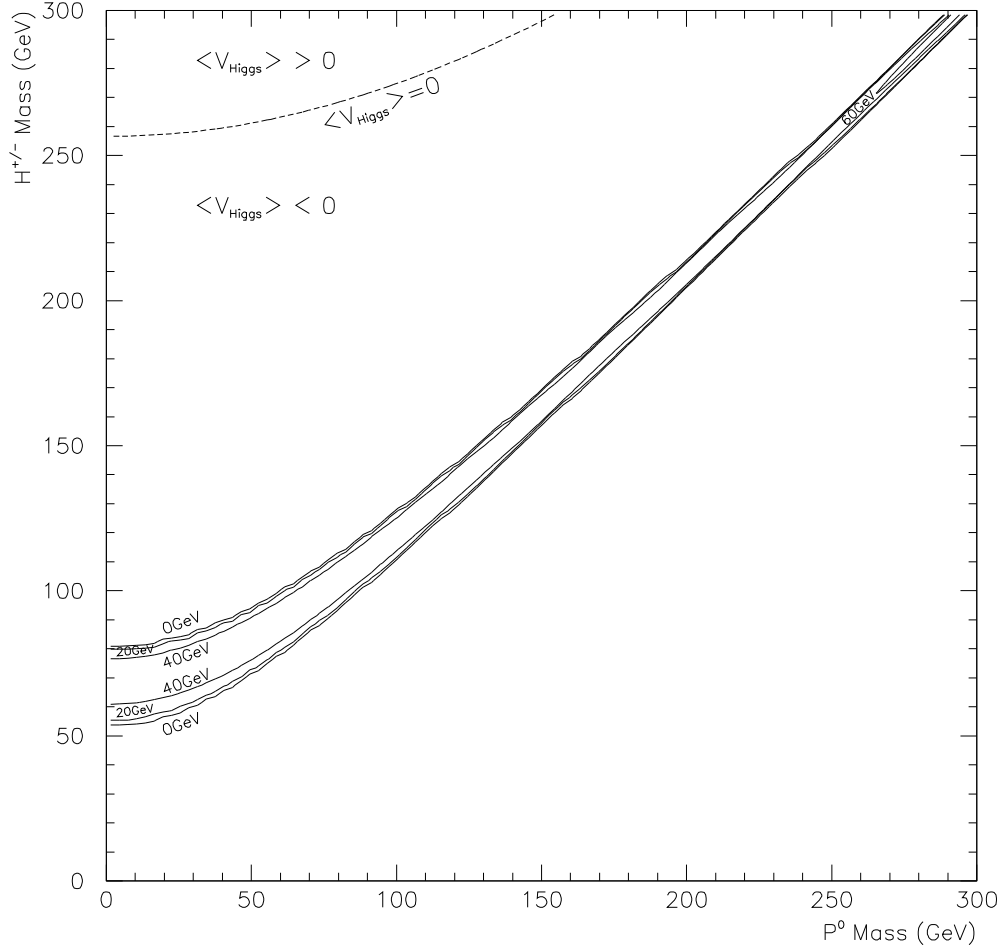


FIG. 9. A plot of the H_1^0 mass contour lines as a function of m_{P^0} and m_{H^\pm} , for $v_1/v_2 = 0.9$ and $v_3/v_2 = 9.1$ ($m_{Z_2} \approx 499 \text{ GeV}$). The dashed curve in the upper left-hand corner is a plot of the zero of the Higgs potential above which it becomes positive.

Finally there is the matter of fixing the heavy fermion masses. The heavy quark masses, $m_{q'}$, will be assumed degenerate as will the charged heavy leptons masses, $m_{l'}$, such that $m_{q',l'} \gtrsim \mathcal{O}(0.1)TeV$ [33]. The e'^{\pm} will be designated to play the role of the charged heavy leptons, L^{\pm} .

Figs. 10 through 16 show the rapidity distribution at $y=0$ for $p\bar{p}^{(\bar{c})} \rightarrow gg \rightarrow L^+L^-$ as function of m_L , for various scenarios. The rapidity distribution, $d\sigma/dy$, is related to the parton level cross-section, $\hat{\sigma}(gg \rightarrow L^+L^-)$, through

$$\frac{d\sigma}{dy} = \int_{\tau_{min}}^{e^{|y|}} d\tau G(\sqrt{\tau}e^y, Q^2)G(\sqrt{\tau}e^{-y}, Q^2)\hat{\sigma}(\tau s), \quad (101)$$

where $\tau = \hat{s}/s$, $\tau_{min} = 4m_L^2/s$, \sqrt{s} is the center-of-mass energy, and $G(x, Q^2)$ is the gluon structure function. The values of \sqrt{s} have been set to $14TeV$ (*LHC*) for Figs. 10- 15, and $1.8TeV$ (*TEVATRON*) for Fig. 16. In these figures the *SM* couplings and masses were extracted from the PDG [33], except for $m_t \approx 180 \pm 12 GeV$ [34]. For $G(x, Q^2)$ the leading order Duke and Owens 1.1 (*DO1.1*) [35,36] gluon distribution was used. The results were compared with the next to leading order *MRSA* [37] gluon distribution function, which yielded a negligible difference. Although these results include squark mixing it was found that there was no significant change if mixing is not included. Since $d\sigma/dy$ is flat about $y = 0$, the relationship between $\frac{d\sigma}{dy}|_{y=0}$ and the total cross-section is immediate. Therefore the total event rate for the $p\bar{p}^{(\bar{c})} \rightarrow gg \rightarrow L^+L^-$ production mechanism can be estimated from $y = 0$,

$$\sigma = \int_{\ln\sqrt{\tau_{min}}}^{-\ln\sqrt{\tau_{min}}} \frac{d\sigma}{dy} dy \approx -\ln(\tau_{min}) \sigma. \quad (102)$$

Figs. 10-12 show $\frac{d\sigma}{dy}|_{y=0}$ for different VEV's ratios along the $m_{Z_2} \approx \mathcal{O}(500) GeV$ contour line of Fig. 6. Notice that as v_1/v_2 becomes comparable to v_3/v_2 the large v_3 limit breaks down and the generally small qP^0 term starts to contribute (the $q(Z_{1,2} - P^0)$ contribution also grows quite significantly but remains a negligible contribution). Therefore for relatively large values of v_1/v_2 variations in m_{P^0} ($\approx m_{H^{\pm}}$ up to at least $\mathcal{O}(1)TeV$) become important. However it is more natural to assume that the intragenerational Yukawa couplings are of the

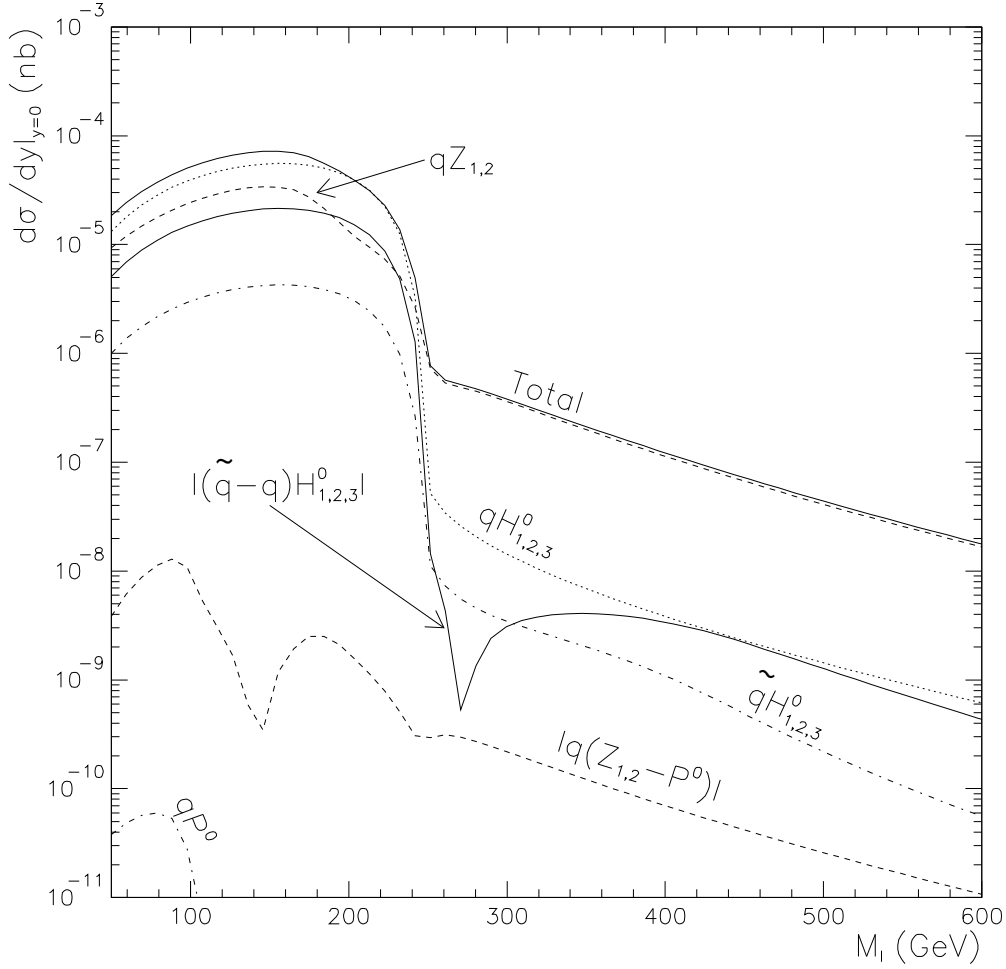


FIG. 10. Rapidity distribution at $y = 0$ for charged heavy lepton production at LHC ($14 TeV$) as a function of heavy lepton mass, where $v_1/v_2 = 0.02$, $v_3/v_2 = 6.7$, and $m_S = 400 GeV$. The mass spectrum for the non-SM particles involved in these processes are, $m_{Z_2} \approx 496 GeV$ ($\Gamma_{Z_2} \approx 20.9 GeV$), $m_{P^0} \approx 200 GeV$ ($\Gamma_{P^0} \approx 16.4 GeV$), $m_{H^\pm} \approx 215 GeV$, $m_{H_1^0} \approx 94.3 GeV$ ($\Gamma_{H_1^0} \approx 7.50 \times 10^{-3} GeV$), $m_{H_2^0} \approx 200 GeV$ ($\Gamma_{H_2^0} \approx 16.5 GeV$), $m_{H_3^0} \approx 495 GeV$ ($\Gamma_{H_3^0} \approx 0.230 GeV$), $m_{q'} = 200 GeV$.

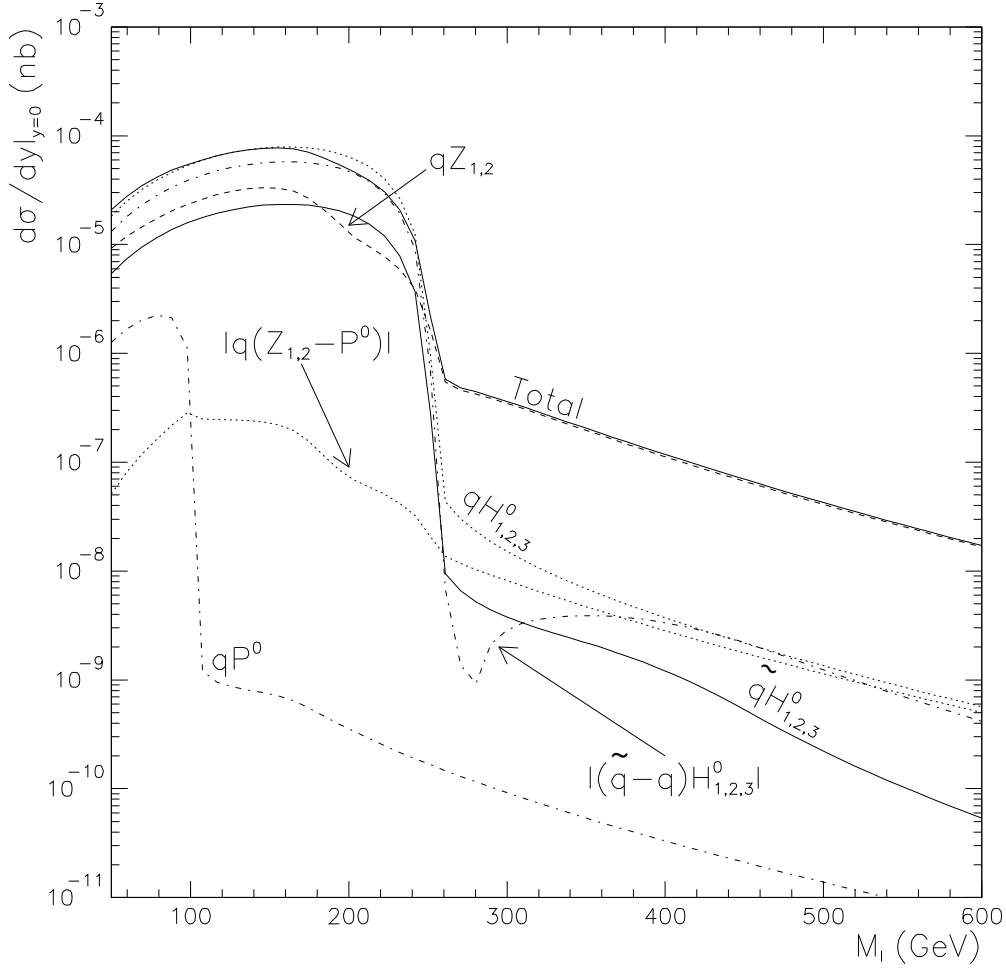


FIG. 11. Rapidity distribution at $y = 0$ for charged heavy lepton production at LHC ($14 TeV$) as a function of heavy lepton mass, where $v_1/v_2 = 0.5$, $v_3/v_2 = 7.7$, and $m_S = 400 GeV$. The mass spectrum for the non-SM particles involved in these processes are, $m_{Z_2} \approx 509 GeV$ ($\Gamma_{Z_2} \approx 21.5 GeV$), $m_{P^0} \approx 200 GeV$ ($\Gamma_{P^0} \approx 2.52 \times 10^{-2} GeV$), $m_{H^\pm} \approx 212 GeV$, $m_{H_1^0} \approx 75.4 GeV$ ($\Gamma_{H_1^0} \approx 3.65 \times 10^{-3} GeV$), $m_{H_2^0} \approx 212 GeV$ ($\Gamma_{H_2^0} \approx 7.49 \times 10^{-2} GeV$), $m_{H_3^0} \approx 507 GeV$ ($\Gamma_{H_3^0} \approx 0.198 GeV$), $m_{q'} = 200 GeV$.

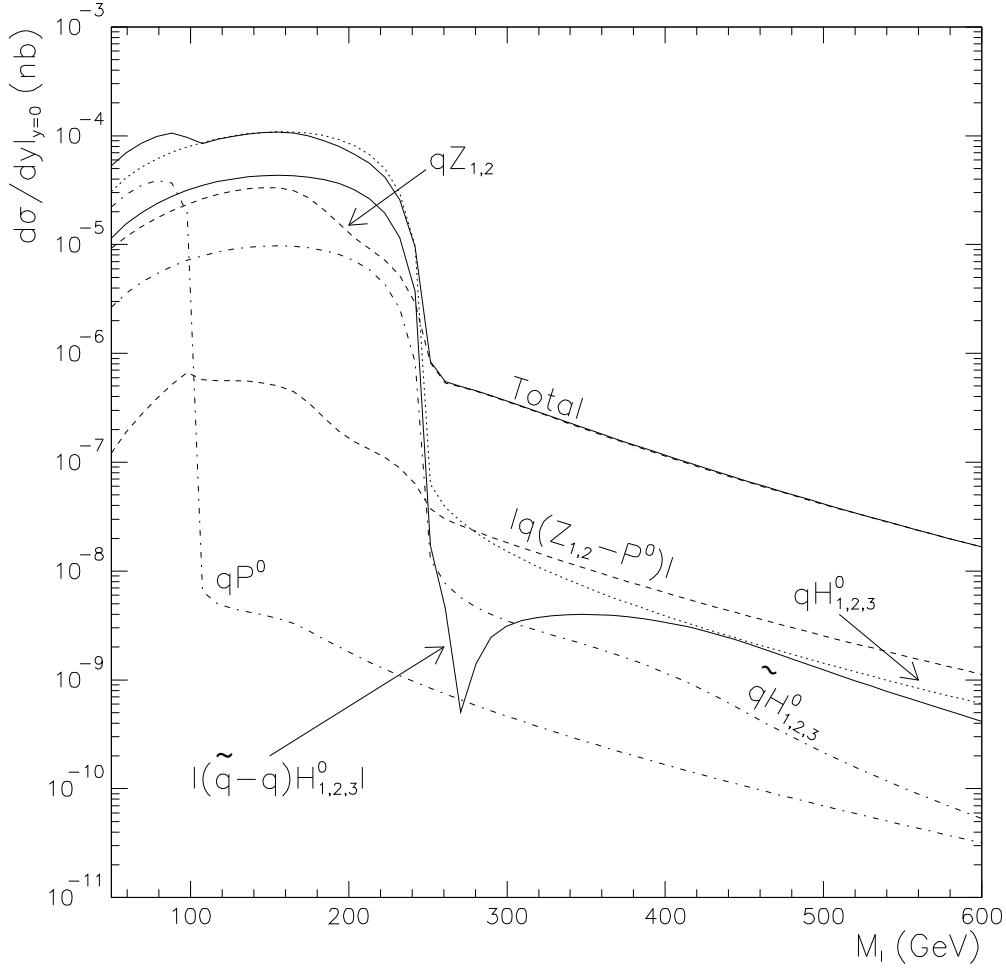


FIG. 12. Rapidity distribution at $y = 0$ for charged heavy lepton production at LHC ($14 TeV$) as a function of heavy lepton mass, where $v_1/v_2 = 0.9$, $v_3/v_2 = 9.1$, and $m_S = 400 GeV$. The mass spectrum for the non-SM particles involved in these processes are, $m_{Z_2} \approx 499 GeV$ ($\Gamma_{Z_2} \approx 20.8 GeV$), $m_{P^0} \approx 200 GeV$ ($\Gamma_{P^0} \approx 8.13 \times 10^{-3} GeV$), $m_{H^\pm} \approx 212 GeV$, $m_{H_1^0} \approx 52.3 GeV$ ($\Gamma_{H_1^0} \approx 1.87 \times 10^{-3} GeV$), $m_{H_2^0} \approx 216 GeV$ ($\Gamma_{H_2^0} \approx 1.37 \times 10^{-2} GeV$), $m_{H_3^0} \approx 498 GeV$ ($\Gamma_{H_3^0} \approx 0.130 GeV$), $m_{q'} = 200 GeV$.

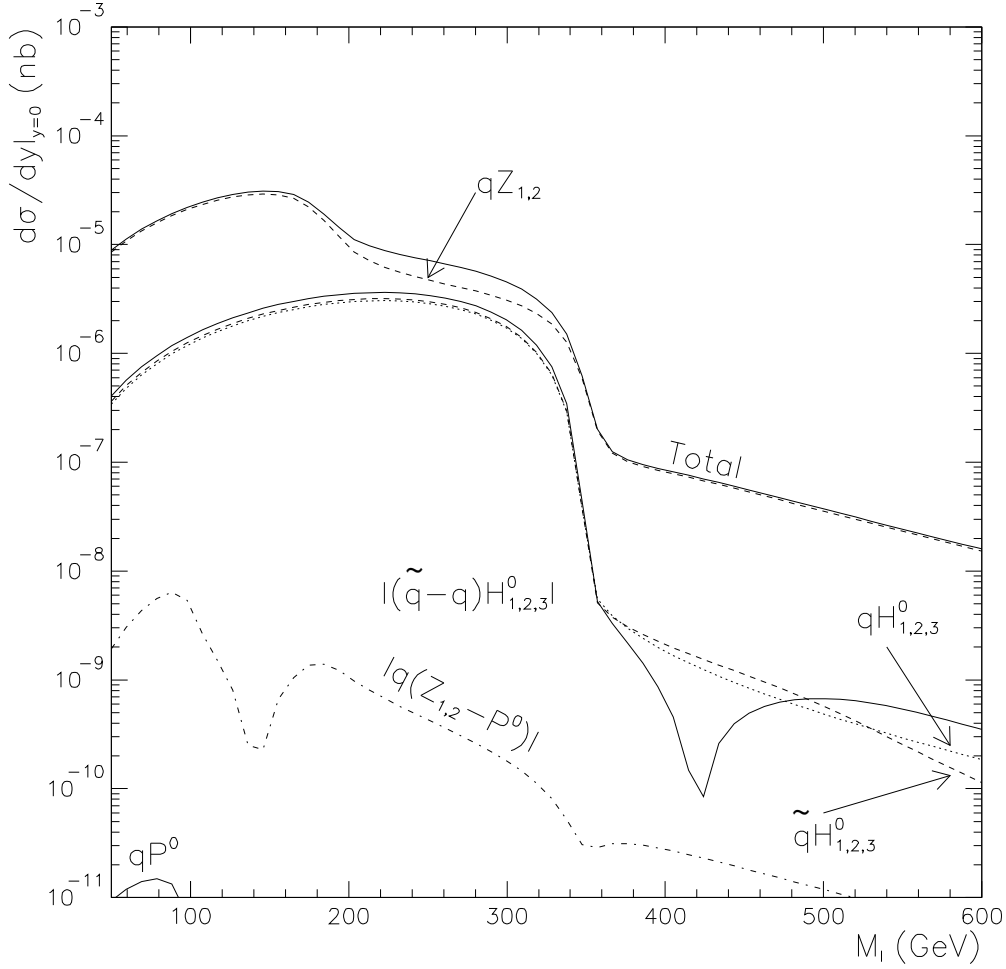


FIG. 13. Rapidity distribution at $y = 0$ for charged heavy lepton production at LHC ($14 TeV$) as a function of heavy lepton mass, where $v_1/v_2 = 0.02$, $v_3/v_2 = 9.5$, and $m_S = 450 GeV$. The mass spectrum for the non-SM particles involved in these processes are, $m_{Z_2} \approx 700 GeV$ ($\Gamma_{Z_2} \approx 31.9 GeV$), $m_{P^0} \approx 200 GeV$ ($\Gamma_{P^0} \approx 16.5 GeV$), $m_{H^\pm} \approx 215 GeV$, $m_{H_1^0} \approx 94.6 GeV$ ($\Gamma_{H_1^0} \approx 7.49 \times 10^{-3} GeV$), $m_{H_2^0} \approx 200 GeV$ ($\Gamma_{H_2^0} \approx 16.5 GeV$), $m_{H_3^0} \approx 700 GeV$ ($\Gamma_{H_3^0} \approx 1.04 GeV$), $m_{q'} = 200 GeV$.

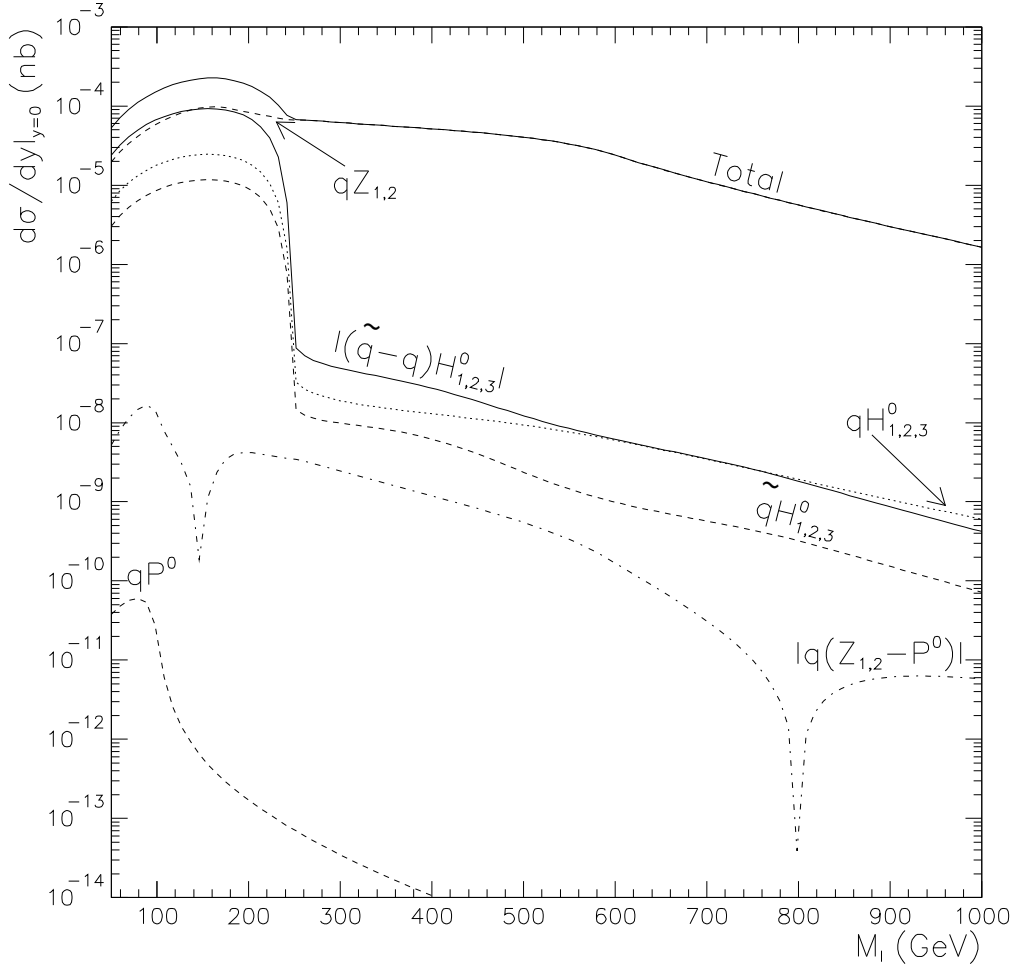


FIG. 14. Rapidity distribution at $y = 0$ for charged heavy lepton production at LHC ($14 TeV$) as a function of heavy lepton mass, where $v_1/v_2 = 0.02$, $v_3/v_2 = 6.7$, and $m_S = 400 GeV$. The mass spectrum is for the non-SM particles involved in these processes are, $m_{Z_2} \approx 496 GeV$ ($\Gamma_{Z_2} \approx 19.4 GeV$), $m_{P^0} \approx 200 GeV$ ($\Gamma_{P^0} \approx 16.4 GeV$), $m_{H^\pm} \approx 215 GeV$, $m_{H_1^0} \approx 94.3 GeV$ ($\Gamma_{H_1^0} \approx 7.50 \times 10^{-3} GeV$), $m_{H_2^0} \approx 200 GeV$ ($\Gamma_{H_2^0} \approx 16.5 GeV$), $m_{H_3^0} \approx 495 GeV$ ($\Gamma_{H_3^0} \approx 0.138 GeV$), $m_{q'} = 600 GeV$.

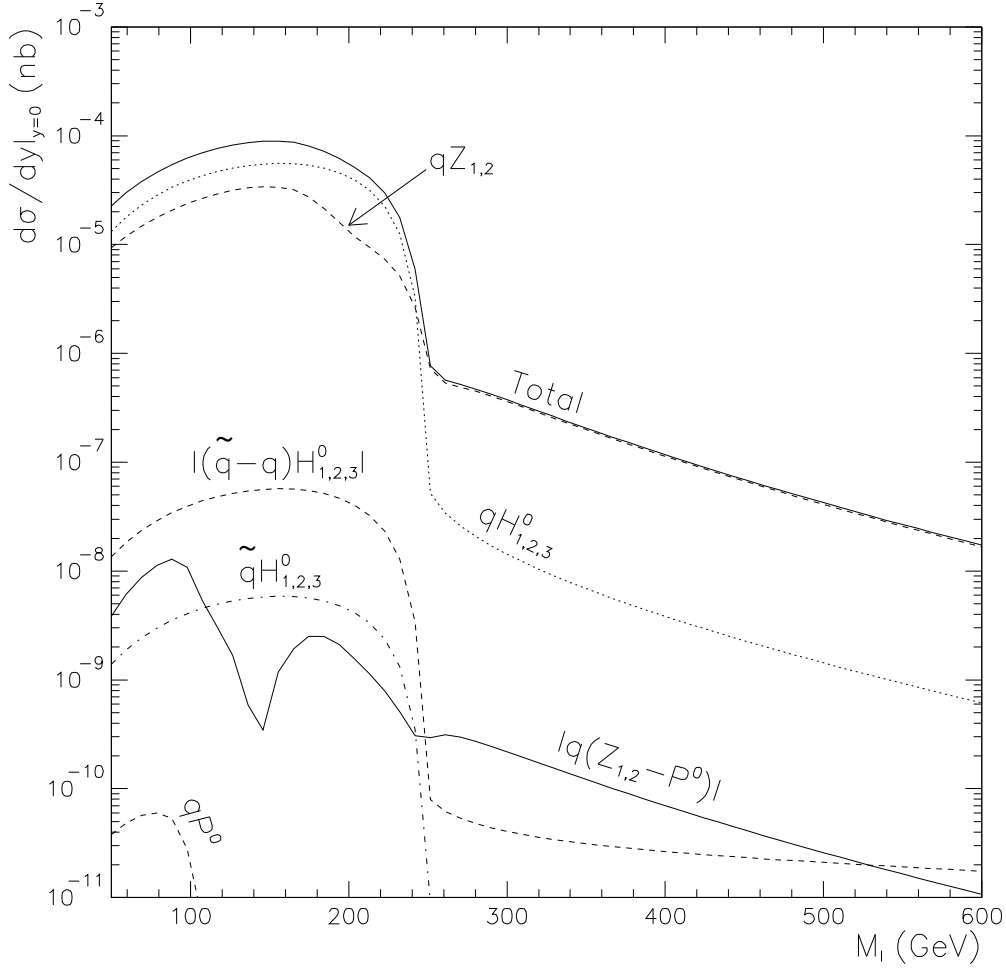


FIG. 15. Rapidity distribution at $y = 0$ for charged heavy lepton production at LHC ($14 TeV$) as a function of heavy lepton mass, where $v_1/v_2 = 0.02$, $v_3/v_2 = 6.7$, and $m_S = 1 TeV$. The mass spectrum for the non-SM particles involved in these processes are, $m_{Z_2} \approx 496 GeV$ ($\Gamma_{Z_2} \approx 20.9 GeV$), $m_{P^0} \approx 200 GeV$ ($\Gamma_{P^0} \approx 16.4 GeV$), $m_{H^\pm} \approx 215 GeV$, $m_{H_1^0} \approx 94.3 GeV$ ($\Gamma_{H_1^0} \approx 7.50 \times 10^{-3} GeV$), $m_{H_2^0} \approx 200 GeV$ ($\Gamma_{H_2^0} \approx 16.5 GeV$), $m_{H_3^0} \approx 495 GeV$ ($\Gamma_{H_3^0} \approx 0.230 GeV$), $m_{q'} = 200 GeV$.

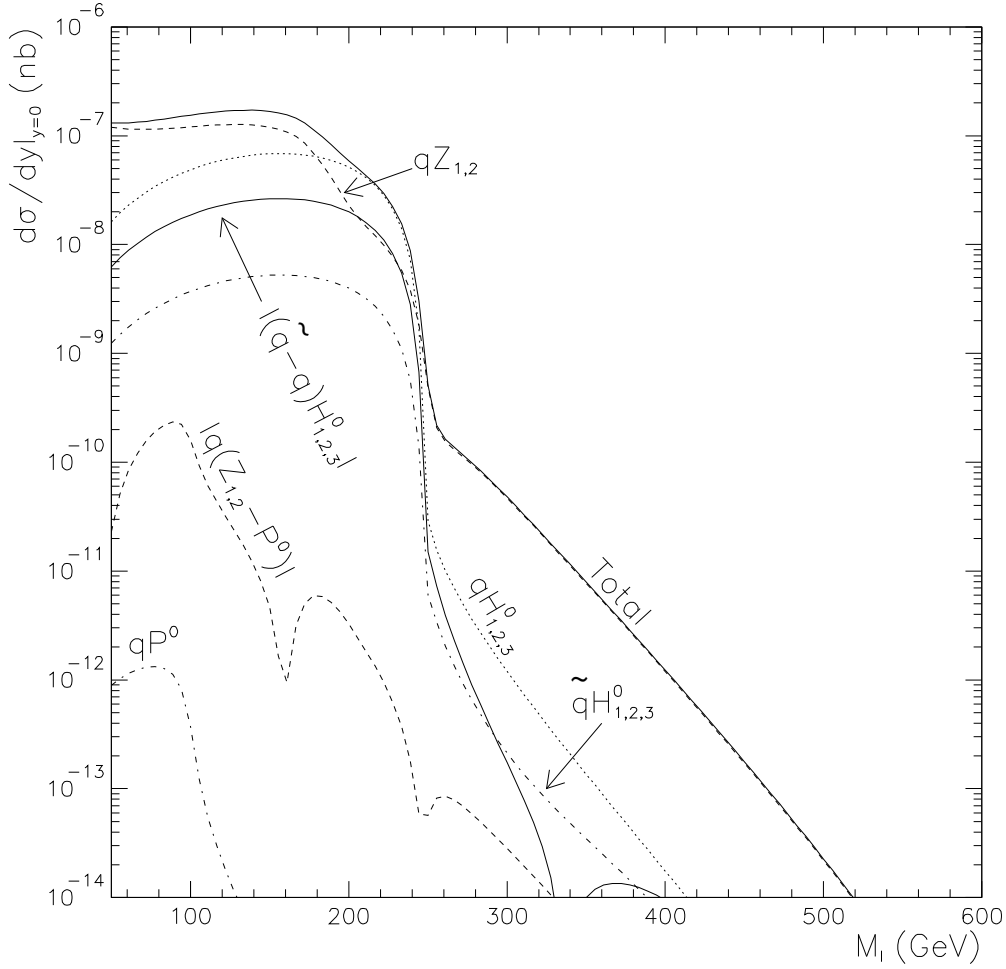


FIG. 16. Rapidity distribution at $y = 0$ for charged heavy lepton production at the TEVATRON (1.8TeV) as a function of heavy lepton mass, where $v_1/v_2 = 0.02$, $v_3/v_2 = 6.7$, and $m_S = 400\text{GeV}$. The mass spectrum for the non-SM particles involved in these processes are, $m_{Z_2} \approx 496\text{GeV}$ ($\Gamma_{Z_2} \approx 20.9\text{GeV}$), $m_{P^0} \approx 200\text{GeV}$ ($\Gamma_{P^0} \approx 16.4\text{GeV}$), $m_{H^\pm} \approx 215\text{GeV}$, $m_{H_1^0} \approx 94.2\text{GeV}$ ($\Gamma_{H_1^0} \approx 7.50 \times 10^{-3}\text{GeV}$), $m_{H_2^0} \approx 200\text{GeV}$ ($\Gamma_{H_2^0} \approx 16.5\text{GeV}$), $m_{H_3^0} \approx 495\text{GeV}$ ($\Gamma_{H_3^0} \approx 0.230\text{GeV}$), $m_{q'} = 200\text{GeV}$.

same order of magnitude and therefore for v_1/v_2 to be small. For the rest of these figures then, it will be assumed that $v_1/v_2 = 0.02$. Fig. 10 is the figure with the default values.

Fig. 13 shows what happens when a larger Z_2 mass of $\mathcal{O}(700 \text{ GeV})$ (*i.e.*, $v_3/v_2 = 9.5$) is used. For this figure m_S had to be pushed up slightly to 450 GeV , in order to produce physical squark masses. The noticeable difference between this and all of the other figures is that the peak has broadened. This is expected since the Z_2 can remain on-shell for larger values of m_L . Notice that the H_3^0 resonance cut off seems to follow the Z_2 's. More precisely, $m_{H_3^0} \approx m_{Z_2}$ for large v_3 . This becomes immediately evident when taking the large v_3 limits of the H_i^0 and Z_i mass mixing matrices, Eqs. (31) and (48) respectively:

$$\lim_{v_3 \rightarrow \infty} m_{H_3^0}^2 = \lim_{v_3 \rightarrow \infty} m_{Z_2}^2 = \frac{25}{36} g'^2 v_3^2 \approx \frac{25}{9} \frac{(v_3/v_2)^2 x_W}{1 + (v_1/v_2)^2} m_Z^2, \quad (103)$$

which is in fairly good agreement with all of the figures. Also the overall production is slightly suppressed due to the smallness of the gluon distribution function at large momentum fraction.

Fig. 14 shows what happens when the heavy quark mass was pushed up to 600 GeV . The effect is quite dramatic. To see why this is so, notice the slight kink in the curve around $m_L \approx 600 \text{ GeV}$. There is also a much more significant kink in all of the other graphs around 200 GeV , *i.e.*, around $m_L \approx m_{q'}$. Further examination of the parton level cross-section shows that kink occurs when the heavy quarks in the loops can no longer be on shell.

In Fig. 15 the scalar mass was pushed up to 1 TeV . Increasing m_S has caused the terms involving the squarks to be suppressed by several orders of magnitude. The difference between the heavy and light squark cases is that, for heavy squarks, the gluon luminosity is relatively small in the kinematical region where the squarks in the loop are on shell. The qH_i^0 term now enhances L^+L^- production, below the $m_{H_3^0}$ threshold, as the destructive interference with $\bar{q}H_i^0$ term, *i.e.*, $(\bar{q} - q)H_i^0$, has been suppressed.

Finally Fig. 16 shows what happens at $\sqrt{s} = 1.8 \text{ TeV}$, the TEVATRON. The overall topology is the same as depicted in Fig. 10 but the L^+L^- production rate is dramatically reduced: very little gluon luminosity is available to produce these heavy particles.

B. Drell-Yan

Fig. 17 shows the Feynman diagrams used for computing the parton level Drell-Yan contribution to heavy lepton production [4,38]. Drell-Yan production of heavy leptons occurs

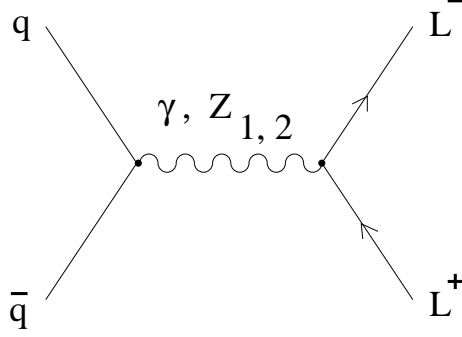


FIG. 17. Feynman diagrams for Drell-Yan production of charged heavy leptons.

through an s -channel γ , Z_1 or Z_2 . The differential cross section for this process can be expressed as follows:

$$\frac{d\hat{\sigma}_{L^\pm}}{d\Omega} = \frac{1}{64\pi^2\hat{s}}\beta \left\{ |\overline{\mathcal{M}_\gamma}|^2 + |\overline{\mathcal{M}_{Z_1}}|^2 + |\overline{\mathcal{M}_{Z_2}}|^2 + 2\text{Re}(\overline{\mathcal{M}_\gamma\mathcal{M}_{Z_1}^\dagger} + \overline{\mathcal{M}_\gamma\mathcal{M}_{Z_2}^\dagger} + \overline{\mathcal{M}_{Z_1}\mathcal{M}_{Z_2}^\dagger}) \right\} \quad (104)$$

The “direct” squared matrix elements (the first three terms in the above expression) are given by

$$|\overline{\mathcal{M}_i}|^2 = \frac{2G_i^4}{(\hat{s} - M_i^2)^2 + \Gamma_i^2 M_i^2} \left\{ 4v_q^i a_q^i v_L^i a_L^i (2m_L^2(\hat{t} - \hat{u}) - (\hat{t}^2 - \hat{u}^2)) \right. \\ \left. + [(v_q^i)^2 + (a_q^i)^2] [(v_L^i)^2 + (a_L^i)^2] (2m_L^2(\hat{s} - m_L^2) + \hat{u}^2 + \hat{t}^2) - [(v_L^i)^2 - (a_L^i)^2] (2m_L^2\hat{s}) \right\} \quad (105)$$

while the interference terms are given by

$$2\text{Re}(\overline{\mathcal{M}_i\mathcal{M}_j}) = \frac{4G_i^2 G_j^2 ((\hat{s} - M_i^2)(\hat{s} - M_j^2) + \Gamma_i M_i \Gamma_j M_j)}{((\hat{s} - M_i^2)^2 + \Gamma_i^2 M_i^2)((\hat{s} - M_j^2)^2 + \Gamma_j^2 M_j^2)} \left\{ (v_q^i v_q^j + a_q^i a_q^j) \right. \\ \times [(v_L^i v_L^j + a_L^i a_L^j)(2m_L^2(\hat{s} - m_L^2) + \hat{u}^2 + \hat{t}^2) - (v_L^i a_L^j - a_L^i v_L^j)(2m_L^2\hat{s})] \\ \left. + (v_q^i a_q^j + a_q^i v_q^j)(v_L^i a_L^j + a_L^i v_L^j)(2m_L^2(\hat{t} - \hat{u}) - (\hat{t}^2 - \hat{u}^2)) \right\}. \quad (106)$$

In the expressions above, i and j can be γ , Z_1 or Z_2 ; M_i and Γ_i are the mass and width of the gauge boson; m_L is the mass of the heavy lepton; $G_\gamma = e$ and $G_{Z_1} = G_{Z_2} = g/\sqrt{1 - x_W}$.

If $i = \gamma$, $v_f^i = Q_f$ and $a_f^i = 0$ for both quarks ($f = q$) or the heavy lepton ($f = L$). If $i = Z_{1,2}$, $v_f^i = (\tilde{C}_R^{fi} + \tilde{C}_L^{fi})/2$ and $a_f^i = (\tilde{C}_R^{fi} - \tilde{C}_L^{fi})/2$, where again $f = (q, L)$ and the couplings $\tilde{C}_{R,L}^{fi}$ are given by Eqs. (85) and (86). Also, \hat{s} , \hat{t} and \hat{u} are the usual parton level process Mandelstam variables: $(m_L^2 - \hat{t}) = \hat{s}(1 - \beta \cos \theta)/2$ and $(m_L^2 - \hat{u}) = \hat{s}(1 + \beta \cos \theta)/2$, where θ is the angle between the outgoing L^- and the incoming quark q .

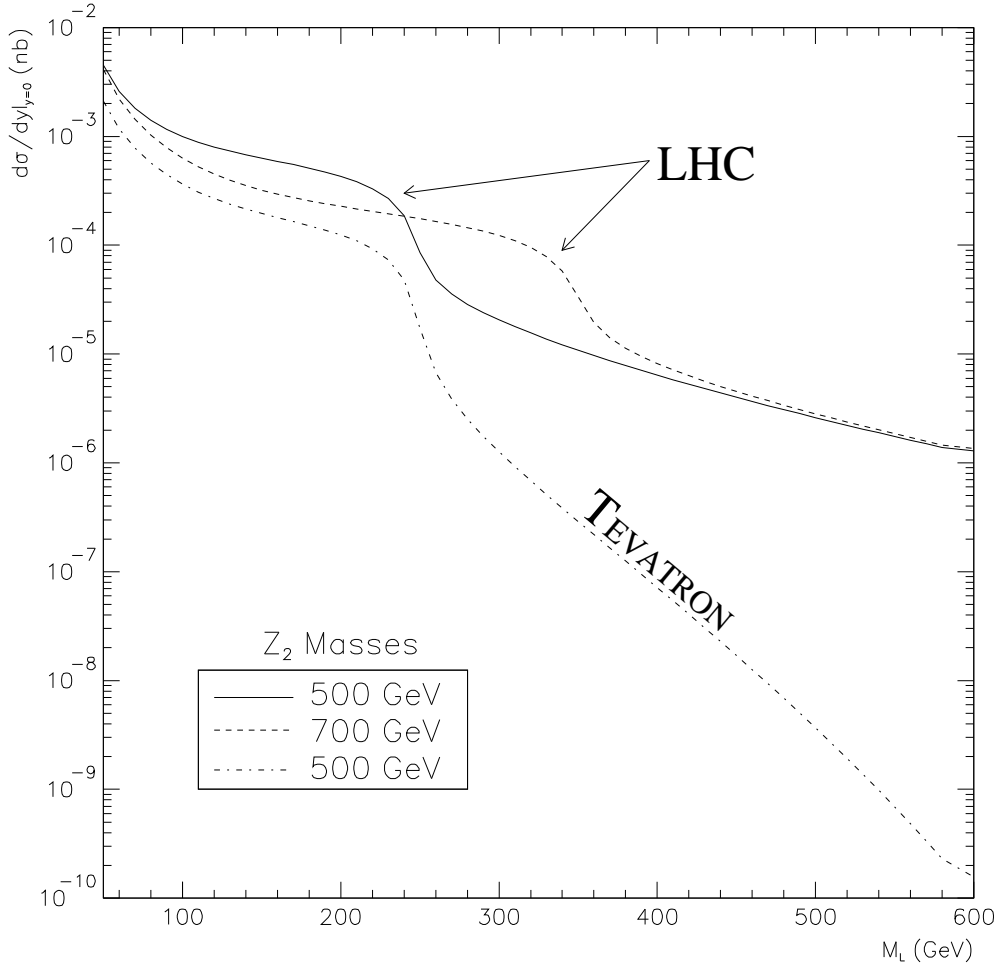


FIG. 18. Drell-Yan rapidity distribution at $y = 0$, as a function of m_L , for L^+L^- production at *LHC* and the *TEVATRON*. The *DO1.1* [35,36] quark and anti-quark parton distribution functions were used to obtain these results.

Fig. 18 shows $d\sigma/dy|_{y=0}$, as a function of m_L , for Drell-Yan production of L^+L^- at *LHC* and the *TEVATRON*. These results are shown for the regions of the E_6 parameter

space that was explored for gluon-gluon fusion, in the previous section: *i.e.*, $m_{Z_2} = 500 \text{ GeV}$ and 700 GeV for *LHC*, and $m_{Z_2} = 500 \text{ GeV}$ for the *TEVATRON*. Notice that Drell-Yan production becomes rapidly suppressed for $2m_L > m_{Z_2}$: the Z_2 must now go off-shell to produce the heavy lepton pairs.

In contrast to gluon-gluon fusion, the *LHC* results for Drell-Yan production are in general, higher by an order of magnitude. For the *TEVATRON* results the difference is quite dramatic! At the *TEVATRON*, a $p\bar{p}$ collider, Drell-Yan production occurs mainly *via* the q and \bar{q} valence partons from the p and \bar{p} , respectively; at the *LHC*, a pp collider, the $\bar{q} \in p$ must come from the sea. The gluon distribution is more similar to sea quark distributions than valence quark distributions, which explains why gluon-gluon fusion is comparable to Drell-Yan production at the *LHC*, but not at the *TEVATRON*.

C. Results

Fig. 19 gives a summary of the total cross-section for L^+L^- production for the E_6 model parameter space studied in the previous sections. At the *TEVATRON* $\mathcal{O}(10^{1\pm 1}) \text{ events/yr}$ are expected for $m_L \lesssim \mathcal{O}(300) \text{ GeV}$, all of it coming from Drell-Yan production (*i.e.*, gluon-gluon fusion yields $\lesssim \mathcal{O}(0.1) \text{ events/yr}$). For *LHC*, over a reasonable range of parameter space, $\mathcal{O}(10^{4\pm 2}) \text{ events/yr}$ are expected.

The charged heavy lepton in the *MSSM* model [27] is a member of a sequential 4th generation added arbitrarily to the model; the lepton masses were chosen larger than 50 GeV and the quarks larger than 150 GeV . For $m_L \lesssim \mathcal{O}(250) \text{ GeV}$ the *LHC* results are comparable in order of magnitude to the *MSSM* predictions, obtained by Cieza Montalvo *et al.* [27], which predicts $\mathcal{O}(10^5) \text{ events/yr}$. However, the dominant mechanism in the *MSSM* model is gluon-gluon fusion and for E_6 this contribution yields $\mathcal{O}(10^{4\pm 1}) \text{ events/yr}$, which is a factor of at least 10 less than *MSSM* results. This is a rather surprising result since it was expected that the E_6 event rate would be enhanced due to the greater number of heavy particles running around in the loop. The parameters in each model were varied to study

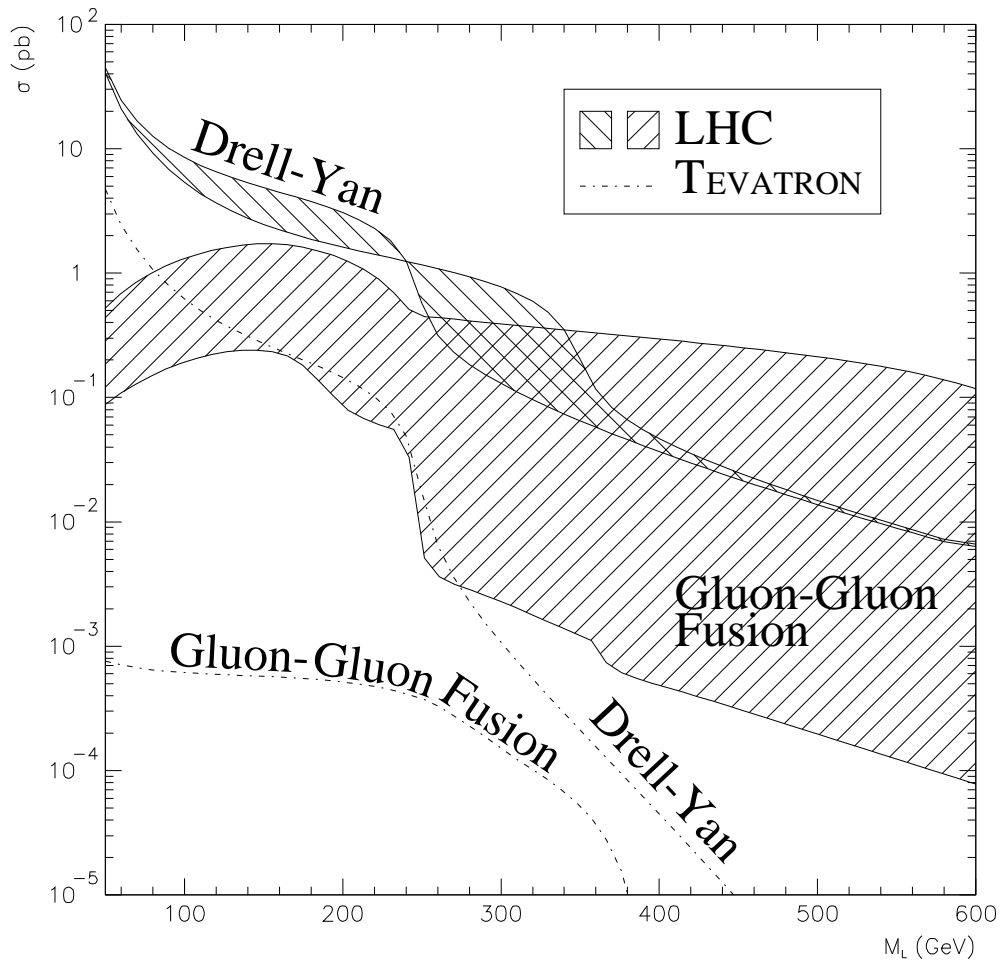


FIG. 19. Summary plot of results for the total L^+L^- production cross-section at LHC ($\sqrt{s} = 14 TeV$, $\mathcal{L} \sim 10^5 pb^{-1}/yr$) and $TEVATRON$ ($\sqrt{s} = 1.8 TeV$, $\mathcal{L} \sim 10^2 pb^{-1}/yr$) energies as a function of m_L . The hatched regions are the LHC results for gluon-gluon fusion, from Figs. 10-15, and Drell-Yan production, from Fig. 18. The dash-dot lines are the $TEVATRON$ results for gluon-gluon fusion, from Fig. 16, and Drell-Yan production, from Fig. 18.

this non-intuitive result. Unfortunately, it turns out that the E_6 parameters suppress L^+L^- production, since v_3 is fairly large. This restriction causes the production to occur mainly through the $Z_{1,2}$ and H_3^0 terms. The $MSSM$ has two neutral Higgses and one pseudo-scalar Higgs that are allowed to contribute to the processes. A very simple test on the E_6 model was done by varying v_3/v_2 , about $v_1/v_2 = 0.2$, that showed for $v_3/v_2 = 2.8$ and $m_L \lesssim 100 \text{ GeV}$ a factor of 10 increase was obtained. However, this region of E_6 parameter space is forbidden, see Fig. 6.

It appears that the Drell-Yan mechanism, used in [27], includes only the the s -channel photon diagram. We find that the inclusion of the Z leads to a factor of 10 increase in the L^+L^- rate, which puts Drell-Yan on equal footing with gluon-gluon fusion for $m_L \lesssim \mathcal{O}(100) \text{ GeV}$, in the $MSSM$ with a fourth generation.

The $L^\pm \rightarrow \nu_L W^\pm, \nu_L H^\pm$ decay modes are expected to be similar for both models, as these are SM-like decays. These modes depend upon the mass difference $\Delta = m_L - m_{\nu_L}$. For $\Delta < m_W \ll m_{H^\pm}$ the decays modes will be by virtual W 's, $W^* \rightarrow f\bar{f}$, and on shell for $\Delta > m_W$. Leptonic decays of the W 's offer the possibility of L^\pm detection by measuring $\ell^+\ell^-$ production with missing transverse momentum, \cancel{p}_T [27]. The competing SM backgrounds with these processes are $pp \rightarrow \tau^+\tau^-$, W^+W^- , Z^0Z^0 . Studies have shown, using SM couplings, that it is possible to pull the L^+L^- signals from background for $\Delta > m_W$ given sufficiently large event rates; it is much more difficult for $\Delta < m_W$ [27,39,40]. In general the $MSSM$ event rate is higher than E_6 , and therefore detection would more likely indicate a $MSSM$ candidate. If $m_{H^\pm} \approx \mathcal{O}(m_W)$, then $H^\pm \rightarrow f_i\bar{f}_j$ dominates, for naturally large values of $\tan\beta$. Since the Higgs likes to couple to massive particles, this would lead multiple heavy jet events which in general would be very difficult to pull out of background in either the $MSSM$ or E_6 . Similar processes are expected to occur for the cases $m_W < \Delta < m_{H^\pm}$ and $m_W, m_{H^\pm} < \Delta$. For large enough m_{H^\pm} , the sfermion channels also open, *i.e.*, $H^\pm \rightarrow \tilde{f}_i\tilde{f}_j^*$ (*e.g.*, $\tilde{u}\tilde{d}^*$). The sfermions would eventually decay out leaving only the lightest supersymmetric particles (LSP 's), which will escape undetected along with the ν_L 's leaving lots of \cancel{p}_T . In fact, all of the aforementioned process will lead to events

with \cancel{p}_T , as the ν_L 's will pass through the detector.

In certain regions of the *MSSM* and E_6 model parameter spaces it may be possible to distinguish between the two models. If L^+L^- event rates are larger than those predicted by E_6 , then the likely candidate is the *MSSM*. Unlike the *MSSM*, it is possible that $m_{H^\pm} < m_W$ in E_6 [4], and therefore if H^\pm 's are found in this mass range the more likely candidate would be E_6 . Another possible way of telling the models apart is to look for sfermion production, $L^\pm \rightarrow f\tilde{f}^*, \tilde{f}\tilde{f}^*$, which is unique to E_6 , since L^\pm has opposite R parity to the other *SM*-like fermions in the $\mathbf{27}$'s (Fig. 1). The sfermion would eventually decay to an *LSP* which is stable (assuming R parity conservation), yielding *jets* + \cancel{p}_T , in general. Whether or not it is possible to distinguish them from the *MSSM* and the *SM*-like backgrounds would require a much more detailed study, as the allowable parameter space for sfermions masses and Yukawa couplings is quite large. Finally, the *MSSM* does have fairly stringent unitarity constraints on the heavy lepton and heavy quark masses as a function of $\tan\beta$ [27], in particular $m_L \lesssim (1200 \text{ GeV}) \cos\beta$. Therefore, it should be possible to eliminate $(m_L, \tan\beta)$ regions in the *MSSM* L^-L^+ production cross-section plots, as a function of m_L , such that only E_6 models are allowed. For example, assuming $m_{H_1^0} \gtrsim \mathcal{O}(600) \text{ GeV}$ rules out the *MSSM* for $m_L \gtrsim 242 \text{ GeV}$ and $\tan\beta \gtrsim 5$. In the allowed *MSSM* region this gives an upper limit on the L^+L^- production cross-section of $\mathcal{O}(10) \text{ pb}$, at *LHC*. Also in the *MSSM* there are phenomenological constraints on $\tan\beta$ which could allow for further restrictions. A more detailed study of these constraints has not been carried out.

In closing, it should be pointed out that only a simple model of E_6 has been considered. It is possible for other E_6 models to produce results similar to the model studied here or to the *MSSM*. Therefore, in general, L^+L^- production by gluon-gluon fusion should not be considered a definitive means of separating out the different models; several experiments would be required.

V. CONCLUSIONS

The $p\bar{p} \rightarrow gg \rightarrow L^+L^-$ production cross-section was computed for a simple rank-5 E_6 model. For a fairly conservative survey of the various parameters in the model we expect $\mathcal{O}(10^{4+2})$ events/yr at *LHC*, and $\mathcal{O}(10^{1\pm 1})$ events/yr at the *TEVATRON*. For *LHC* and the *TEVATRON* it was found that Drell-Yan production dominated over gluon-gluon fusion for $2m_L \leq m_{Z_2}$. For the *TEVATRON* events are only expected to be seen for $2m_L \lesssim \mathcal{O}(m_{Z_2})$, as the Drell-Yan and gluon-gluon fusion rates drop rapidly beyond this point. The *LHC* results were compared to the *MSSM*'s ($\mathcal{O}(10^5)$ events/yr [27]), in which gluon-gluon fusion is the dominant production mode. The gluon-gluon fusion contribution to L^+L^- production at *LHC* ($\mathcal{O}(10^{4\pm 1})$) was found to be at least a factor of 10 less than the event rates predicted for the *MSSM*, due the *CDF* and $D\emptyset$ soft limits (*i.e.*, assuming SM couplings) placed on m_{Z_2} [32]. These soft constraints resulted in the $H_{1,2}^0$ and P^0 contributions to the L^+L^- production rate to be suppressed leaving only the H_3^0 and $Z_{1,2}$ to contribute. For certain regions in the *MSSM* and E_6 parameter spaces it was demonstrated that it is possible to distinguish between the two models, in principle. However, it should be pointed out that there are many candidate E_6 models which could yield overlapping results.

VI. ACKNOWLEDGEMENTS

The authors would like to thank Alan Dekok for proof-reading our pre-print drafts. The computing facilities utilized herein were provided by Carleton University's, Department of Physics, CRPP, OPAL, and THEORY groups, as well as UQAM's Département de Physique. This research was funded by *NSERC* of Canada and *FCAR* du Quebec.

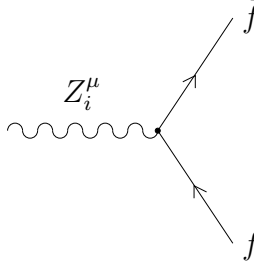
APPENDIX A: COUPLINGS AND WIDTHS FOR $\hat{\sigma}(GG \rightarrow L^+L^-)$

This appendix gives a summary of the calculations that were used to obtain the couplings and the widths for the $\hat{\sigma}(gg \rightarrow L^+L^-)$ matrix elements given in § IV.

1. The Couplings

In this section the calculations of the vertex factors used to obtain the $gg \rightarrow L^+L^-$ matrix elements, given in § IV, are summarized.

For the $Z_{1,2}$ exchange diagrams shown in Fig. 5(a) the following vertex factors were used



$$\frac{-g}{\sqrt{1-x_W}} \gamma^\mu [\tilde{C}_L^{fZ_i} P_L + \tilde{C}_R^{fZ_i} P_R], \quad (\text{A1})$$

where $i = 1, 2$,

$$P_L = \frac{1}{2}(1 - \gamma_5), \quad (\text{A2})$$

$$P_R = \frac{1}{2}(1 + \gamma_5), \quad (\text{A3})$$

and $C_L^{qZ_i}$ and $C_R^{qZ_i}$ were the couplings used in Eq. (83). The gauge-fermion interaction Lagrangian for $\text{SU}(2)_L \otimes \text{U}(1)_Y \otimes \text{U}(1)_E$ is given by

$$\mathcal{L}_{\text{int}} \supseteq -\frac{1}{2} (g_L \hat{\tau}_{ij}^a L_\mu^a + g_Y \delta_{ij} \hat{Y}_{Y_i} Y_\mu + g_E \hat{Y}_{E_i} E_\mu) \bar{\psi}_i \bar{\sigma}^\mu \psi_j, \quad (\text{A4})$$

where the ψ_i 's are two-component spinors, see Eq. (B.2) of Haber and Kane (HK) [16].

Defining $g = g_L$, $g' = g_Y$, $g'' = g_E$, and $\hat{Y} = \hat{Y}_{Y_i} (= 2\hat{Q} - \hat{\tau}_3)$, and using the identities

$$aL_\mu^3 + bY_\mu = (a \cos \theta_W - b \sin \theta_W) Z_\mu + (a \sin \theta_W + b \cos \theta_W) A_\mu, \quad (\text{A5})$$

$$E_\mu = Z'_\mu, \quad (\text{A6})$$

then Eq. (A4) becomes

$$\mathcal{L}_{\text{int}} \supseteq -\left\{ \frac{g}{\cos \theta_W} (\hat{T}_3 - \hat{Q} x_W) Z_\mu + \frac{1}{2} g'' \hat{Y}_E Z'_\mu \right\}_{ij} [\bar{\psi}_{(f_L)_i} \bar{\sigma}^\mu \psi_{(f_L)_j} + \bar{\psi}_{(f_L^c)_i} \bar{\sigma}^\mu \psi_{(f_L^c)_j}], \quad (\text{A7})$$

where $\hat{T}_3 = \hat{\tau}_3/2$, $\tau_i = \sigma_i$, $\tan \theta_W = g'/g$, and $x_W = \sin^2 \theta_W$. Noting that

$$(\hat{T}_3 - \hat{Q} x_W) |f_L^c\rangle = -(\hat{T}_3 - \hat{Q} x_W) |f_R\rangle, \quad (\text{A8})$$

$$\hat{Y}_E |f_L^c\rangle = -\hat{Y}_E |f_R\rangle, \quad (\text{A9})$$

yields

$$\mathcal{L}_{\text{int}} \supseteq - \left\{ \frac{g}{\cos \theta_W} (\hat{T}_3 - \hat{Q} x_W) Z_\mu + \frac{1}{2} g'' \hat{Y}_E Z'_\mu \right\}_{ij} [\bar{\psi}_{(f_L)_i} \bar{\sigma}^\mu \psi_{(f_L)_j} - \bar{\psi}_{(f_R)_i} \bar{\sigma}^\mu \psi_{(f_R)_j}]. \quad (\text{A10})$$

Using the following identities

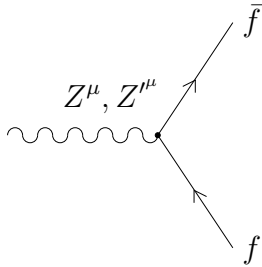
$$\bar{\psi}_{(f_L)_i} \bar{\sigma}^\mu \psi_{(f_L)_j} = \bar{f}_i \gamma^\mu P_L f_j, \quad (\text{A11})$$

$$-\bar{\psi}_{(f_R)_i} \bar{\sigma}^\mu \psi_{(f_R)_j} = \bar{f}_i \gamma^\mu P_R f_j, \quad (\text{A12})$$

to convert from two-component to four-component spinor notation yields

$$\mathcal{L}_{\text{int}} \supseteq \frac{-g}{\sqrt{1-x_W}} \sum_{A=L,R} \bar{f} \left\{ (T_{3A} - e_f x_W) \not{Z} + \frac{1}{2} \left(\frac{g''}{g} \right) y'_{fA} \sqrt{1-x_W} \not{Z}' \right\} P_A f, \quad (\text{A13})$$

see Eqs. (A.28) of HK [16]. Then the Z - Z' -vertex factor is



$$\frac{-g}{\sqrt{1-x_W}} \gamma^\mu [C_L^{fZ, fZ'} P_L + C_R^{fZ, fZ'} P_R], \quad (\text{A14})$$

where the $C_{L,R}^{fZ, fZ'}$'s are defined by Eqs. (85) and (86). Using the inverse of transformations (2) and (3),

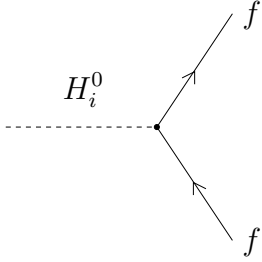
$$\begin{pmatrix} \tilde{Z}' \\ Z \end{pmatrix} = \begin{pmatrix} \cos \phi & -\sin \phi \\ \sin \phi & \cos \phi \end{pmatrix} \begin{pmatrix} Z_1 \\ Z_2 \end{pmatrix}, \quad (\text{A15})$$

yields the desired result

$$\mathcal{L}_{\text{int}} \supseteq \frac{-g}{\sqrt{1-x_W}} \sum_{i=1}^2 \sum_{A=L,R} \bar{f} Z_i \tilde{C}_A^{fZ_i} P_A f, \quad (\text{A16})$$

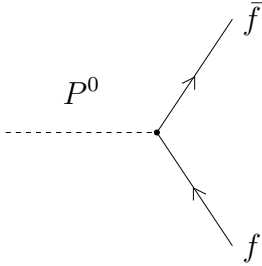
i.e., vertex factor A1.

For the $H_{1,2,3}^0$ and P^0 exchange diagrams shown in Fig. 5(b) the following vertex factors were used



$$-g \frac{m_f}{2m_W} K^{fH_i^0}, \quad (\text{A17})$$

and



$$ig \frac{m_f}{2m_W} \gamma_5 K^{fP^0}, \quad (\text{A18})$$

respectively, where $i = 1, 2, 3$. The $K^{fH_i^0}$ and K^{fP^0} couplings are obtained from the Yukawa interaction part of the Lagrangian given by Eq. (8): noting that $\varepsilon_{ij} = (i\tau_3)_{ij}$ and plugging W, Eq. (7), into Eq. (8) yields

$$\begin{aligned} \mathcal{L}_{Yuk} \supseteq & -\frac{1}{2}\varepsilon_{ij}\{-\lambda_1[\Phi_{2_i}(\psi_{Q_j}\psi_{u_L^c} + \psi_{u_L^c}\psi_{Q_j}) + \Phi_{2_i}^*(\bar{\psi}_{Q_j}\bar{\psi}_{u_L^c} + \bar{\psi}_{u_L^c}\bar{\psi}_{Q_j})] \\ & + \lambda_2[\Phi_{1_i}(\psi_{Q_j}\psi_{d_L^c} + \psi_{d_L^c}\psi_{Q_j}) + \Phi_{1_i}^*(\bar{\psi}_{Q_j}\bar{\psi}_{d_L^c} + \bar{\psi}_{d_L^c}\bar{\psi}_{Q_j})] \\ & + \lambda_3[\Phi_{1_i}(\psi_{L_j}\psi_{e_L^c} + \psi_{e_L^c}\psi_{L_j}) + \Phi_{1_i}^*(\bar{\psi}_{L_j}\bar{\psi}_{e_L^c} + \bar{\psi}_{e_L^c}\bar{\psi}_{L_j})] \\ & + \lambda_4[\Phi_3(\psi_{R'_i}\psi_{L'_j} + \psi_{L'_j}\psi_{R'_i}) + \Phi_3^*(\bar{\psi}_{R'_i}\bar{\psi}_{L'_j} + \bar{\psi}_{L'_j}\bar{\psi}_{R'_i})] \\ & + \lambda_5[\Phi_3(\psi_{d'_L^c}\psi_{d'_L} + \psi_{d'_L}\psi_{d'_L^c}) + \Phi_3^*(\bar{\psi}_{d'_L^c}\bar{\psi}_{d'_L} + \bar{\psi}_{d'_L}\bar{\psi}_{d'_L^c})]\}, \end{aligned} \quad (\text{A19})$$

$$\begin{aligned} \supseteq & -\frac{1}{2}\{\lambda_1[\phi_2^0(\psi_{u_L}\psi_{u_L^c} + \psi_{u_L^c}\psi_{u_L}) + \phi_2^{0*}(\bar{\psi}_{u_L}\bar{\psi}_{u_L^c} + \bar{\psi}_{u_L^c}\bar{\psi}_{u_L})] \\ & + \lambda_2[\phi_1^0(\psi_{d_L}\psi_{d_L^c} + \psi_{d_L^c}\psi_{d_L}) + \phi_1^{0*}(\bar{\psi}_{d_L}\bar{\psi}_{d_L^c} + \bar{\psi}_{d_L^c}\bar{\psi}_{d_L})] \\ & + \lambda_3[\phi_1^0(\psi_{e_L}\psi_{e_L^c} + \psi_{e_L^c}\psi_{e_L}) + \phi_1^{0*}(\bar{\psi}_{e_L}\bar{\psi}_{e_L^c} + \bar{\psi}_{e_L^c}\bar{\psi}_{e_L})] \\ & + \lambda_4[\phi_3^0(\psi_{e'_L}\psi_{e'_L} + \psi_{e'_L}\psi_{e'_L}) + \phi_3^{0*}(\bar{\psi}_{e'_L}\bar{\psi}_{e'_L} + \bar{\psi}_{e'_L}\bar{\psi}_{e'_L})] \\ & + \lambda_5[\phi_3^0(\psi_{d'_L^c}\psi_{d'_L} + \psi_{d'_L}\psi_{d'_L^c}) + \phi_3^{0*}(\bar{\psi}_{d'_L^c}\bar{\psi}_{d'_L} + \bar{\psi}_{d'_L}\bar{\psi}_{d'_L^c})]\}, \end{aligned} \quad (\text{A20})$$

and similarly for the other generations. Defining

$$f = \begin{pmatrix} \psi_{f_L} \\ \bar{\psi}_{f_L^c} \end{pmatrix} \quad (\text{A21})$$

and using the following identities

$$\psi_{f_{1L}^c} \psi_{f_{2L}} = \psi_{f_{2L}} \psi_{f_{1L}^c} = \bar{f}_1 P_L f_2, \quad (\text{A22})$$

$$\bar{\psi}_{f_{1L}^c} \bar{\psi}_{f_{2L}} = \bar{\psi}_{f_{2L}} \bar{\psi}_{f_{1L}^c} = \bar{f}_2 P_R f_1, \quad (\text{A23})$$

see Eqs. (A.24), (A.25), and (A.28) of HK [16], implies

$$\mathcal{L}_{Yuk} \sim -\lambda_i (\phi_j^0 \psi_{f_L^c} \psi_{f_L} + \phi_j^{0*} \bar{\psi}_{f_L^c} \bar{\psi}_{f_L}), \quad (\text{A24})$$

$$= -\frac{1}{2} \lambda_i [\phi_j^0 \bar{f}(1 - \gamma_5) f + \phi_j^{0*} \bar{f}(1 + \gamma_5) f], \quad (\text{A25})$$

$$= -\lambda_i [\text{Re}(\phi_j^0) \bar{f} f - i \text{Im}(\phi_j^0) \bar{f} \gamma_5 f], \quad (\text{A26})$$

$$= -\frac{1}{\sqrt{2}} \lambda_i (\phi_{jR}^0 \bar{f} f - i \phi_{jI}^0 \bar{f} \gamma_5 f). \quad (\text{A27})$$

Expanding the ϕ_i^0 's in terms of their physical fields, Eqs. (40)-(45), yields

$$\begin{aligned} \mathcal{L}_{Yuk} \supseteq & \underbrace{-\frac{1}{\sqrt{2}} \{ \lambda_1 \nu_2 \bar{u} u + \lambda_2 \nu_1 \bar{d} d + \lambda_3 \nu_1 \bar{e} e + \lambda_4 \nu_3 \bar{e}' e' + \lambda_5 \nu_3 \bar{d}' d' \}}_{\text{Eq. (55)}} \\ & - \frac{1}{\sqrt{2}} \sum_{j=1}^3 \{ \lambda_1 U_{2j} \bar{u} u + U_{1j} (\lambda_2 \bar{d} d + \lambda_3 \bar{e} e) + U_{3j} (\lambda_4 \bar{e}' e' + \lambda_5 \bar{d}' d') \} H_j^0 \\ & + \frac{i\kappa}{\sqrt{2}} \{ \lambda_1 \nu_{13} \bar{u} \gamma_5 u + \nu_{23} (\lambda_2 \bar{d} \gamma_5 d + \lambda_3 \bar{e} \gamma_5 e) + \nu_{12} (\lambda_4 \bar{e}' \gamma_5 e' + \lambda_5 \bar{d}' \gamma_5 d') \} P^0, \quad (\text{A28}) \end{aligned}$$

The couplings can now be read directly and give, *via* Eqs. (56)-(60),

$$K^{uH_i^0} = \frac{1}{\sin \beta} U_{2i}, \quad (\text{A29})$$

$$K^{dH_i^0} = \frac{1}{\cos \beta} U_{1i}, \quad (\text{A30})$$

$$K^{d'H_i^0} = \frac{2m_W}{g\nu_3} U_{3i}, \quad (\text{A31})$$

$$K^{eH_i^0} = \frac{1}{\cos\beta} U_{1i}, \quad (\text{A32})$$

$$K^{e'H_i^0} = \frac{2m_W}{g\nu_3} U_{3i}, \quad (\text{A33})$$

for the scalar Higgs fields, H_i^0 , and

$$K^{uP^0} = \frac{1}{\sin\beta} \kappa\nu_{13}, \quad (\text{A34})$$

$$K^{dP^0} = \frac{1}{\cos\beta} \kappa\nu_{23}, \quad (\text{A35})$$

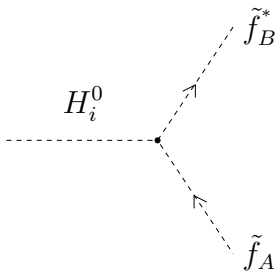
$$K^{d'P^0} = \frac{2m_W}{g\nu_3} \kappa\nu_{12}, \quad (\text{A36})$$

$$K^{eP^0} = \frac{1}{\cos\beta} \kappa\nu_{23}, \quad (\text{A37})$$

$$K^{e'P^0} = \frac{2m_W}{g\nu_3} \kappa\nu_{12}, \quad (\text{A38})$$

for pseudo-scalar Higgs fields, P^0 .

For the $H_{1,2,3}^0$ exchange diagrams shown in Figs. 5(c) and 5(d) the following vertex factors were used



$$\kappa_{AB}^{\tilde{H}_i^0} = -\frac{gm_Z}{\sqrt{1-x_W}} K_{AB}^{\tilde{H}_i^0}, \quad (\text{A39})$$

where $A, B = L, R$. The $\kappa_{AB}^{\tilde{H}_i^0}$ couplings, which were obtained from Eq. (9), are as follows:

$$\begin{aligned}\kappa_{LL}^{\tilde{u}H_i^0} &= \left(\frac{1}{18}g''^2 - \frac{1}{4}g + \frac{1}{12}g'^2\right) U_{1i} \nu_1 + \left(\frac{2}{9}g''^2 + \frac{1}{4}g - \frac{1}{12}g'^2 - \lambda_1^2\right) U_{2i} \nu_2 \\ &\quad - \frac{5}{18}g''^2 U_{3i} \nu_3,\end{aligned}\tag{A40}$$

$$\begin{aligned}\kappa_{RR}^{\tilde{u}H_i^0} &= \left(\frac{1}{18}g''^2 - \frac{1}{3}g'^2\right) U_{1i} \nu_1 + \left(\frac{2}{9}g''^2 + \frac{1}{3}g'^2 - \lambda_1^2\right) U_{2i} \nu_2 \\ &\quad - \frac{5}{18}g''^2 U_{3i} \nu_3,\end{aligned}\tag{A41}$$

$$\kappa_{LR}^{\tilde{u}H_i^0} = \frac{1}{2} [(U_{3i} \nu_1 + U_{1i} \nu_3)\lambda - \sqrt{2} U_{2i} A_u] \lambda_1,\tag{A42}$$

$$\begin{aligned}\kappa_{LL}^{\tilde{d}H_i^0} &= \left(\frac{1}{18}g''^2 + \frac{1}{4}g + \frac{1}{12}g'^2 - \lambda_2^2\right) U_{1i} \nu_1 + \left(\frac{2}{9}g''^2 - \frac{1}{4}g - \frac{1}{12}g'^2\right) U_{2i} \nu_2 \\ &\quad - \frac{5}{18}g''^2 U_{3i} \nu_3,\end{aligned}\tag{A43}$$

$$\begin{aligned}\kappa_{RR}^{\tilde{d}H_i^0} &= -\left(\frac{1}{36}g''^2 - \frac{1}{6}g'^2 + \lambda_2^2\right) U_{1i} \nu_1 - \left(\frac{1}{9}g''^2 + \frac{1}{6}g'^2\right) U_{2i} \nu_2 \\ &\quad + \frac{5}{36}g''^2 U_{3i} \nu_3,\end{aligned}\tag{A44}$$

$$\kappa_{LR}^{\tilde{d}H_i^0} = \frac{1}{2} [(U_{3i} \nu_2 + U_{2i} \nu_3)\lambda - \sqrt{2} U_{1i} A_d] \lambda_2,\tag{A45}$$

$$\begin{aligned}\kappa_{LL}^{\tilde{d}'H_i^0} &= -\left(\frac{1}{9}g''^2 + \frac{1}{6}g'^2\right) U_{1i} \nu_1 - \left(\frac{4}{9}g''^2 - \frac{1}{6}g'^2\right) U_{2i} \nu_2 \\ &\quad + \left(\frac{5}{9}g''^2 - \lambda_5^2\right) U_{3i} \nu_3,\end{aligned}\tag{A46}$$

$$\begin{aligned}\kappa_{RR}^{\tilde{d}'H_i^0} &= -\left(\frac{1}{36}g''^2 - \frac{1}{6}g'^2\right) U_{1i} \nu_1 - \left(\frac{1}{9}g''^2 + \frac{1}{6}g'^2\right) U_{2i} \nu_2 \\ &\quad + \left(\frac{5}{36}g''^2 - \lambda_5^2\right) U_{3i} \nu_3,\end{aligned}\tag{A47}$$

$$\kappa_{LR}^{\tilde{d}'H_i^0} = \frac{1}{2} [(U_{2i} \nu_1 + U_{1i} \nu_2)\lambda - \sqrt{2} U_{3i} A_{d'}] \lambda_5,\tag{A48}$$

for the squark-Higgs couplings, and

$$\begin{aligned}\kappa_{LL}^{\tilde{e}H_i^0} &= -\left(\frac{1}{18}g''^2 - \frac{1}{4}g + \frac{1}{4}g'^2 + \lambda_3^2\right) U_{1i} \nu_1 - \left(\frac{2}{9}g''^2 + \frac{1}{4}g - \frac{1}{4}g'^2\right) U_{2i} \nu_2 \\ &\quad + \frac{5}{36}g''^2 U_{3i} \nu_3,\end{aligned}\tag{A49}$$

$$\begin{aligned}\kappa_{RR}^{\tilde{e}H_i^0} &= \left(\frac{1}{18}g''^2 + \frac{1}{2}g'^2 - \lambda_3^2\right) U_{1i} \nu_1 + \left(\frac{2}{9}g''^2 - \frac{1}{2}g'^2\right) U_{2i} \nu_2 \\ &\quad - \frac{5}{18}g''^2 U_{3i} \nu_3,\end{aligned}\tag{A50}$$

$$\kappa_{LR}^{\tilde{e}H_i^0} = \frac{1}{2} [(U_{3i} \nu_2 + U_{2i} \nu_3)\lambda - \sqrt{2} U_{1i} A_e] \lambda_2,\tag{A51}$$

$$\begin{aligned}\kappa_{LL}^{\tilde{\nu}_e H_i^0} &= -\left(\frac{1}{36}g''^2 + \frac{1}{4}g + \frac{1}{4}g'^2\right) U_{1i} \nu_1 - \left(\frac{1}{9}g''^2 - \frac{1}{4}g - \frac{1}{4}g'^2\right) U_{2i} \nu_2 \\ &\quad + \frac{5}{36}g''^2 U_{3i} \nu_3,\end{aligned}\tag{A52}$$

$$\kappa_{RR}^{\tilde{\nu}_e H_i^0} = \frac{5}{36}g''^2 (U_{1i} \nu_1 + 4U_{2i} \nu_2 - 5U_{3i} \nu_3),\tag{A53}$$

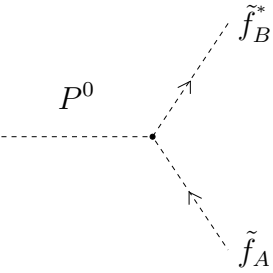
$$\kappa_{LR}^{\tilde{\nu}_e H_i^0} = 0, \quad (\text{A54})$$

for the slepton-Higgs couplings. The mass eigenstate couplings $\tilde{K}_{1,2}^{\tilde{f}H_i^0}$, given by Eqs. (90) and (91), were obtained by inserting

$$\begin{pmatrix} \tilde{f}_L \\ \tilde{f}_R \end{pmatrix} = \begin{pmatrix} \cos \theta_{\tilde{f}} & -\sin \theta_{\tilde{f}} \\ \sin \theta_{\tilde{f}} & \cos \theta_{\tilde{f}} \end{pmatrix} \begin{pmatrix} \tilde{f}_1 \\ \tilde{f}_2 \end{pmatrix}, \quad (\text{A55})$$

which is just the inverse of Eq. (78), into the scalar potential.

The corresponding pseudo-scalar-Higgses couplings



$$i \kappa_{AB}^{\tilde{d} P^0} = -i \frac{gm_Z}{\sqrt{1-x_W}} K_{AB}^{\tilde{q} P^0} \quad (\text{A56})$$

are obtained in a similar fashion as above: *i.e.*,

$$\kappa_{AB}^{\tilde{u} P^0} = -\epsilon_{AB} \frac{\nu_2}{2\sqrt{\nu_{12}^2 + \nu^2 \nu_3^2}} \left[(\nu_1^2 + \nu_3^2)\lambda + \sqrt{2} A_u \nu_3 \cot \beta \right] \lambda_1, \quad (\text{A57})$$

$$\kappa_{AB}^{\tilde{d} P^0} = -\epsilon_{AB} \frac{\nu_1}{2\sqrt{\nu_{12}^2 + \nu^2 \nu_3^2}} \left[(\nu_2^2 + \nu_3^2)\lambda + \sqrt{2} A_d \nu_3 \tan \beta \right] \lambda_2, \quad (\text{A58})$$

$$\kappa_{AB}^{\tilde{d} P^0} = -\epsilon_{AB} \frac{\nu_3}{2\sqrt{\nu_{12}^2 + \nu^2 \nu_3^2}} \left[\nu^2 \lambda + \sqrt{2} A_d \frac{\nu_{12}}{\nu_3} \right] \lambda_5, \quad (\text{A59})$$

for squark-pseudo-Higgs couplings, and

$$\kappa_{AB}^{\tilde{e} P^0} = -\epsilon_{AB} \frac{\nu_1}{2\sqrt{\nu_{12}^2 + \nu^2 \nu_3^2}} \left[(\nu_2^2 + \nu_3^2)\lambda + \sqrt{2} A_e \nu_3 \tan \beta \right] \lambda_3, \quad (\text{A60})$$

$$\kappa_{AB}^{\tilde{\nu}_e P^0} = 0, \quad (\text{A61})$$

for the slepton-pseudo-Higgs couplings, where

$$\epsilon_{AB} = \begin{cases} 1 & \text{if } A = L, B = R \\ 0 & \text{if } A = B \\ -1 & \text{if } A = R, B = L \end{cases}. \quad (\text{A62})$$

In general, these couplings will also mix to give the mass eigenstate couplings $\tilde{K}_{1,2}^{fP^0}$; which are defined in a similar fashion to Eqs. (90) and (91).

2. The Widths

In this section all of the tree level two-body decay widths for Z_2 , H_i^0 , and P_0 are computed. Therefore the generic two body decay formula is given by [41]

$$\Gamma = \frac{S|\mathcal{M}_{ab}|^2}{16\pi m_0} \beta_{ab}, \quad \begin{array}{c} \uparrow m_a \\ \bigcirc m_0 \\ \downarrow m_b \end{array} \quad (\text{A63})$$

where m_i , $i = 0, a, b$, are the masses of the particles, p_i , in the decay process $p_0 \rightarrow p_a p_b$,

$$\beta_{ab} = \sqrt{1 - \frac{2(m_a^2 + m_b^2)}{m_0^2} + \frac{(m_a^2 - m_b^2)^2}{m_0^4}}, \quad (\text{A64})$$

such that $\beta_{ab} \equiv \beta_a$ if $a = b$, S is a symmetry factor for the out going particles, p_a and p_b , and \mathcal{M}_{ab} is the amplitude for the process.

a. Γ_{Z_2}

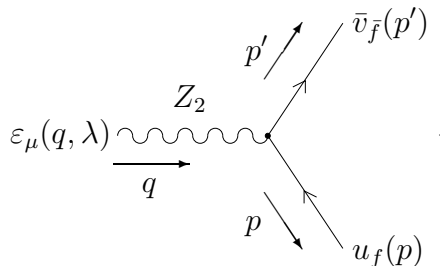
For the Z_2 width, the following processes need to be computed:

$$Z_2 \longrightarrow W^+W^-, Z_1H_i^0, W^\pm H^\mp, q_i\bar{q}_i, l_i\bar{l}_i, \tilde{\chi}_i^0\tilde{\chi}_j^0, \tilde{\chi}_i^+\tilde{\chi}_j^-, \tilde{q}_i\tilde{q}_j^*, \tilde{l}_i\tilde{l}_j^*, H_i^0H_j^0, H^+H^-, P^0H_i^0.$$

The $Z_2 \rightarrow W^+W^-$ width, which can be found in Hewett and Rizzo [4], is given by

$$\Gamma(Z_2 \rightarrow W^+W^-) = \frac{g^2 m_{Z_2} \sin^2 \phi}{192\pi(1 - x_W)} \left(\frac{m_{Z_2}}{m_Z}\right)^4 \beta_W^3 \left[1 + 20 \left(\frac{m_W}{m_Z}\right)^2 + 12 \left(\frac{m_W}{m_Z}\right)^4\right]. \quad (\text{A65})$$

The $Z_2 \rightarrow q_i\bar{q}_i, l_i\bar{l}_i$ vertex factors are given by



$$-g\gamma_\mu(v_f - a_f\gamma_5), \quad (\text{A66})$$

which were obtained from Eq. (A16) by converting to the $V - A$ basis: *i.e.*,

$$a P_L + b P_R = v_f - a_f \gamma_5, \quad (\text{A67})$$

where

$$v_f = \frac{1}{2} (a + b), \quad (\text{A68})$$

$$a_f = \frac{1}{2} (a - b), \quad (\text{A69})$$

which yields

$$v_f = \frac{1}{2\sqrt{1-x_W}} (\tilde{C}_L^{fZ_2} + \tilde{C}_R^{fZ_2}), \quad (\text{A70})$$

$$a_f = \frac{1}{2\sqrt{1-x_W}} (\tilde{C}_L^{fZ_2} - \tilde{C}_R^{fZ_2}). \quad (\text{A71})$$

Therefore

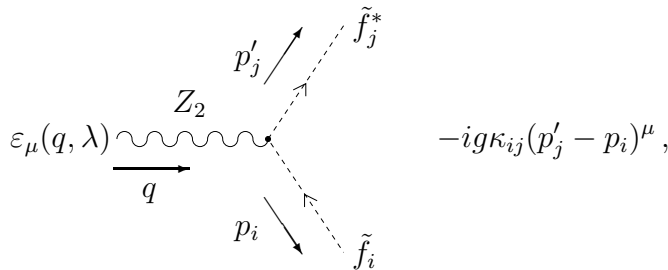
$$\begin{aligned} |\overline{\mathcal{M}_{f\bar{f}}}|^2 &= \frac{1}{3} g^2 \sum_{\lambda} \sum_{spin} |\bar{v}(p') \gamma_{\mu} (v_f - a_f \gamma_5) u(p) \varepsilon^{\mu}(q, \lambda)|^2, \\ &= \frac{4}{3} g^2 [v_f^2 (m_{Z_2}^2 + 2m_f^2) + a_f^2 (m_{Z_2}^2 - 4m_f^2)]. \end{aligned} \quad (\text{A72})$$

Plugging this into Eq. (A63) gives

$$\Gamma(Z_2 \rightarrow f\bar{f}) = c_f \frac{g^2}{12\pi} m_{Z_2} \beta_f \left[v_f^2 \left(1 + \frac{2m_f^2}{m_{Z_2}^2} \right) + a_f^2 \left(1 - \frac{4m_f^2}{m_{Z_2}^2} \right) \right], \quad (\text{A73})$$

where c_f is a colour factor which is 3 for quarks and 1 for leptons.

The $Z_2 \rightarrow \tilde{q}_i \tilde{q}_j^*, \tilde{l}_i \tilde{l}_j^*$ vertex factors are given by



$$-ig \kappa_{ij} (p'_j - p_i)^{\mu}, \quad (\text{A74})$$

where $\tilde{f}_{k=1,2}$ are sfermion mass eigenstates, and

$$\kappa_{ij} = \begin{cases} v_f + a_f \cos 2\theta_{\tilde{f}} & ; \text{ if } i = j = 1 \\ v_f - a_f \cos 2\theta_{\tilde{f}} & ; \text{ if } i = j = 2 \\ -a_f \sin 2\theta_{\tilde{f}} & ; \text{ if } i \neq j \end{cases} . \quad (\text{A75})$$

The vertex factor is obtained by follow steps similar to Eqs. (A4)-(A16),

$$\mathcal{L}_{\text{int}} \supseteq -\frac{i}{2} (g_L \hat{\tau}_{ij}^a L_\mu^a + g_Y \delta_{ij} \hat{Y}_{Y_i} Y_\mu + g_E \hat{Y}_{E_i} E_\mu) \tilde{f}_i^* \overleftrightarrow{\partial}^\mu \tilde{f}_j \quad (\text{A76})$$

$$\supseteq \frac{-ig}{\sqrt{1-x_W}} \sum_{i=1}^2 \sum_{A=L,R} \tilde{C}_A^{fZ_i} \tilde{f}_A^* \overleftrightarrow{\partial}_\mu \tilde{f}_A Z_i^\mu , \quad (\text{A77})$$

followed by transforming the sfermions to their mass eigenstates by using Eq. (A55),

$$\begin{aligned} \mathcal{L}_{\text{int}} \supseteq & \frac{-ig}{\sqrt{1-x_W}} \sum_{i=1}^2 \{ [\tilde{C}_L^{fZ_i} \cos^2 \theta_{\tilde{f}} + \tilde{C}_R^{fZ_i} \sin^2 \theta_{\tilde{f}}] \tilde{f}_1^* \overleftrightarrow{\partial}_\mu \tilde{f}_1 \\ & + [\tilde{C}_L^{fZ_i} \sin^2 \theta_{\tilde{f}} + \tilde{C}_R^{fZ_i} \cos^2 \theta_{\tilde{f}}] \tilde{f}_2^* \overleftrightarrow{\partial}_\mu \tilde{f}_2 \\ & - \frac{1}{2} [\tilde{C}_L^{fZ_i} - \tilde{C}_R^{fZ_i}] \sin 2\theta_{\tilde{f}} (\tilde{f}_1^* \overleftrightarrow{\partial}_\mu \tilde{f}_2 + \tilde{f}_2^* \overleftrightarrow{\partial}_\mu \tilde{f}_1) \} Z_i^\mu , \end{aligned} \quad (\text{A78})$$

and then changing to the $V - A$ basis, *via* Eqs. (A67)-(A71), to get

$$\mathcal{L}_{\text{int}} \supseteq -ig \sum_{i,j,k=1}^2 \kappa_{ij} \tilde{f}_i^* \overleftrightarrow{\partial}_\mu \tilde{f}_j Z_k^\mu . \quad (\text{A79})$$

Therefore

$$\begin{aligned} \overline{|\mathcal{M}_{\tilde{f}_i \tilde{f}_j^*}|^2} &= \frac{1}{3} g^2 \sum_{\lambda} |\varepsilon_\mu(q, \lambda) \kappa_{ij} (p'_j - p_i)^\mu|^2 , \\ &= \frac{1}{3} g^2 m_{Z_2}^2 \kappa_{ij}^2 \beta_{\tilde{f}_i \tilde{f}_j}^2 . \end{aligned} \quad (\text{A80})$$

Plugging this into Eq. (A63) gives

$$\Gamma(Z_2 \rightarrow \tilde{f}_i \tilde{f}_j^*) = c_f \frac{g^2 m_{Z_2}}{48\pi} \kappa_{ij}^2 \beta_{\tilde{f}_i \tilde{f}_j}^2 . \quad (\text{A81})$$

For the range of VEV's that will be consider here (*i.e.*, large v_3 in particular) the $Z_2 \rightarrow Z_1 H_i^0, W^\pm H^\mp, H_i^0 H_j^0, H^+ H^- , P^0 H_i^0$ widths can be approximated by

$$\Gamma(Z_2 \rightarrow V + S) \approx \frac{17g^2 x_W}{864\pi(1-x_W)} m_{Z_2} , \quad (\text{A82})$$

where the $H_i^0 H_j^0$ contributions are kinematically forbidden or suppressed [4].

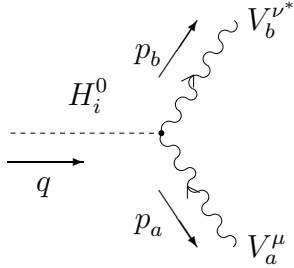
The $Z_2 \rightarrow \tilde{\chi}_i^0 \tilde{\chi}_j^0, \tilde{\chi}_i^+ \tilde{\chi}_j^-$ widths are quite difficult to compute, due to the complex nature of the mass matrices, and can contribute as much as 10-20% to the total width, neglecting phase space suppression [4]. Here its contribution will be taken as 15%; this approximation proved to have no noticeable impact on $L^+ L^-$ production.

b. $\Gamma_{H_i^0}$

For the H_i^0 widths the following processes need to be computed:

$$H_i^0 \longrightarrow Z_j Z_k, W^+ W^-, q_j \bar{q}_j, l_j \bar{l}_j, \tilde{\chi}_j^0 \tilde{\chi}_k^0, \tilde{\chi}_j^+ \tilde{\chi}_k^-, \tilde{q}_j \tilde{q}_k^*, \tilde{l}_j \tilde{l}_k^*, H_j^0 H_k^0, H^+ H^-, P^0 P^0.$$

The $H_i^0 \rightarrow Z_j Z_k, W^+ W^-$ vertex factors are given by



$$i C_{V_a V_b}^{H_i^0} g_{\mu\nu}, \quad (\text{A83})$$

where

$$C_{Z_1 Z_1}^{H_i^0} = C_{Z Z}^{H_i^0} \cos^2 \phi - 2 C_{Z Z'}^{H_i^0} \sin 2\phi + C_{Z' Z'}^{H_i^0} \sin^2 \phi, \quad (\text{A84})$$

$$C_{Z_1 Z_2}^{H_i^0} = C_{Z Z'}^{H_i^0} \cos 2\phi - (C_{Z Z}^{H_i^0} - C_{Z' Z'}^{H_i^0}) \sin 2\phi, \quad (\text{A85})$$

$$C_{Z_2 Z_2}^{H_i^0} = C_{Z Z}^{H_i^0} \sin^2 \phi + 2 C_{Z Z'}^{H_i^0} \sin 2\phi + C_{Z' Z'}^{H_i^0} \cos^2 \phi, \quad (\text{A86})$$

for the Z_i 's, with

$$C_{Z Z}^{H_i^0} = \frac{1}{4} (g \cos \theta_W + g' \sin \theta_W)^2 (U_{1i} v_1 + U_{2i} v_2), \quad (\text{A87})$$

$$C_{Z Z'}^{H_i^0} = \frac{g''}{6} (g \cos \theta_W + g' \sin \theta_W) (U_{1i} v_1 - 4 U_{2i} v_2), \quad (\text{A88})$$

$$C_{Z' Z'}^{H_i^0} = \frac{g''^2}{36} (U_{1i} v_1 + 16 U_{2i} v_2 + 25 U_{3i} v_3), \quad (\text{A89})$$

and

$$C_{W^+W^-}^{H_i^0} = \frac{g^2}{2} (U_{1i}v_1 + U_{2i}v_2), \quad (\text{A90})$$

for the W 's. The vertex factors, $C_{V_a V_b}^{H_i^0}$, were obtained by plugging Eq. (A15) and Eqs. (40)-(45) into the kinetic terms for the scalar-Higgs fields, Eq. (23). Therefore

$$\begin{aligned} \overline{|\mathcal{M}_{ab}^i|^2} &= \sum_{\lambda_a \lambda_b} |\varepsilon_\mu(p_a, \lambda_a) C_{V_a V_b}^{H_i^0} \varepsilon_\nu^*(p_b, \lambda_b) g^{\mu\nu}|^2 \\ &= \frac{m_{H_i^0}^4 C_{V_a V_b}^{H_i^0}{}^2}{4(m_a m_b)^2} \left[1 - \frac{2(m_a^2 + m_b^2)}{m_{H_i^0}^2} + \frac{(m_a^2 + m_b^2)^2 + 8(m_a m_b)^2}{m_{H_i^0}^4} \right], \end{aligned} \quad (\text{A91})$$

which yields, *via* Eq. (A63),

$$\Gamma(H_i^0 \rightarrow V_a V_b) = \frac{S C_{V_a V_b}^{H_i^0}{}^2 m_{H_i^0}^3 \beta_{ab}}{64\pi(m_a m_b)^2} \left[1 - \frac{2(m_a^2 + m_b^2)}{m_{H_i^0}^2} + \frac{(m_a^2 + m_b^2)^2 + 8(m_a m_b)^2}{m_{H_i^0}^4} \right], \quad (\text{A92})$$

where $S = \frac{1}{2}$ for identical Z_i 's, otherwise $S = 1$.

The $H_i^0 \rightarrow q_i \bar{q}_i, l_i \bar{l}_i$ decay width is

$$\Gamma(H_i^0 \rightarrow f \bar{f}) = \frac{c_f g^2}{32\pi} \left(\frac{m_f}{m_W} \right)^2 K^{fH_i^0}{}^2 \beta_{H_i^0}^3 m_{H_i^0}, \quad (\text{A93})$$

via Eq. (A63) with amplitude

$$\overline{|\mathcal{M}_{f\bar{f}}|^2} = \frac{g^2}{2} \left(\frac{m_f}{m_W} \right)^2 K^{fH_i^0}{}^2 [m_{H_i^0}^2 - 4m_f^2], \quad (\text{A94})$$

where the $K^{fH_i^0}$ couplings are defined by Eq. (A17).

For the scalar processes $H_i^0 \rightarrow \tilde{\phi} \phi^*$ the vertex factor is



$$C_{\phi_a \phi_b}^{H_i^0}, \quad (\text{A95})$$

which yields the decay width

$$\Gamma(H_i^0 \rightarrow \phi_a \phi_b^*) = \frac{c_f}{16\pi m_{H_i^0}} |C_{\phi_a \phi_b}^{H_i^0}|^2 \beta_{ab}, \quad (\text{A96})$$

via Eq. (A63), with amplitude

$$\overline{|\mathcal{M}_{\phi_a\phi_b}|^2} = |C_{\phi_a\phi_b}^{H_i^0}|^2. \quad (\text{A97})$$

For $H_i^0 \rightarrow \tilde{q}_j \tilde{q}_k^*, \tilde{l}_j \tilde{l}_k^*$ the vertex factors are

$$C_{\tilde{f}_j \tilde{f}_k^*}^{H_i^0} = \frac{g m_Z}{\sqrt{1-x_W}} K_{jk}^{\tilde{f}H_i^0}, \quad (\text{A98})$$

where the $K_{jk}^{\tilde{f}H_i^0}$ couplings are given by Eqs. (A29)-(A33). For $H_i^0 \rightarrow H_j^0 H_k^0, H^+ H^-, P^0 P^0$ the vertex factors are:

$$\begin{aligned} C_{H_1^0 H_1^0}^{H_2^0} &= \frac{1}{2} \lambda A (U_{12} U_{21} U_{31} + U_{11} U_{22} U_{31} + U_{11} U_{21} U_{32}) \\ &+ \left\{ U_{12} \left[\frac{-1}{24} (g''^2 + 9g^2 + 9g'^2) U_{11}^2 - \left(\frac{1}{18} g''^2 - \frac{1}{8} g^2 - \frac{1}{8} g'^2 \right) U_{21}^2 \right. \right. \\ &+ \left. \frac{5}{72} g''^2 U_{31}^2 - \frac{1}{2} \lambda^2 (U_{21}^2 + U_{31}^2) \right] + U_{11} \left[\left(\frac{-1}{18} g''^2 + \frac{1}{8} g^2 + \frac{1}{8} g'^2 \right) U_{21} U_{22} \right. \\ &+ \left. \left. \frac{5}{36} g''^2 U_{31} U_{32} - \lambda^2 (U_{21} U_{22} + U_{31} U_{32}) \right] \right\} v_1 \\ &+ \left\{ U_{22} \left[\left(\frac{-1}{18} g''^2 + \frac{1}{8} g^2 + \frac{1}{8} g'^2 \right) U_{11}^2 - \frac{1}{24} (16g''^2 + 9g^2 + 9g'^2) U_{21}^2 \right. \right. \\ &+ \left. \frac{5}{18} g''^2 U_{31}^2 - \frac{1}{2} \lambda^2 (U_{11}^2 + U_{31}^2) \right] + U_{21} \left[\left(\frac{-1}{9} g''^2 + \frac{1}{4} g^2 + \frac{1}{4} g'^2 \right) U_{11} U_{12} \right. \\ &+ \left. \left. \frac{5}{9} g''^2 U_{31} U_{32} - \lambda^2 (U_{11} U_{12} + U_{31} U_{32}) \right] \right\} v_2 \\ &+ \left\{ U_{31} \left[\frac{5}{36} g''^2 (U_{11} U_{12} + 4U_{21} U_{22}) - \lambda^2 (U_{11} U_{12} + U_{21} U_{22}) \right] \right. \\ &+ \left. U_{32} \left[\frac{5}{72} g''^2 (U_{11}^2 + 4U_{21}^2 - 15U_{31}^2) - \frac{1}{2} (U_{11}^2 + U_{21}^2) \right] \right\} v_3, \quad (\text{A99}) \end{aligned}$$

$$\begin{aligned} C_{H_1^0 H_1^0}^{H_3^0} &= \frac{1}{2} \lambda A (U_{13} U_{21} U_{31} + U_{11} U_{23} U_{31} + U_{11} U_{21} U_{33}) \\ &+ \left\{ U_{13} \left[\frac{-1}{24} (g''^2 + 9g^2 + 9g'^2) U_{11}^2 - \left(\frac{1}{18} g''^2 - \frac{1}{8} g^2 - \frac{1}{8} g'^2 \right) U_{21}^2 \right. \right. \\ &+ \left. \frac{5}{72} g''^2 U_{31}^2 - \frac{1}{2} \lambda^2 (U_{21}^2 + U_{31}^2) \right] + U_{11} \left[\left(\frac{-1}{9} g''^2 + \frac{1}{4} g^2 + \frac{1}{4} g'^2 \right) U_{21} U_{23} \right. \\ &+ \left. \left. \frac{5}{36} g''^2 U_{31} U_{33} - \lambda^2 (U_{21} U_{23} + U_{31} U_{33}) \right] \right\} v_1 \\ &+ \left\{ U_{23} \left[\left(\frac{-1}{18} g''^2 + \frac{1}{8} g^2 + \frac{1}{8} g'^2 \right) U_{11}^2 - \frac{1}{24} (16g''^2 + 9g^2 + 9g'^2) U_{21}^2 \right. \right. \\ &+ \left. \frac{5}{18} g''^2 U_{31}^2 - \frac{1}{2} \lambda^2 (U_{11}^2 + U_{31}^2) \right] + U_{21} \left[\left(\frac{-1}{9} g''^2 + \frac{1}{4} g^2 + \frac{1}{4} g'^2 \right) U_{11} U_{13} \right. \\ &+ \left. \left. \frac{5}{9} g''^2 U_{31} U_{33} - \lambda^2 (U_{11} U_{13} + U_{31} U_{33}) \right] \right\} v_2 \end{aligned}$$

$$\begin{aligned}
& + \left\{ U_{31} \left[\frac{5}{36} g''^2 (U_{11} U_{13} + 4U_{21} U_{23}) - \lambda^2 (U_{11} U_{13} + U_{21} U_{23}) \right] \right. \\
& + U_{33} \left[\frac{5}{72} g''^2 (U_{11}^2 + 4U_{21}^2 - 15U_{31}^2) - \frac{1}{2} (U_{11}^2 + U_{21}^2) \right] \left. \right\} v_3, \tag{A100}
\end{aligned}$$

$$\begin{aligned}
C_{H_1^0 H_2^0}^{H_3^0} = & \frac{1}{2} \lambda A (U_{13} U_{22} U_{31} + U_{12} U_{23} U_{31} + U_{13} U_{21} U_{32} \\
& + U_{11} U_{23} U_{32} + U_{12} U_{21} U_{33} + U_{11} U_{22} U_{33}) \\
& - \left\{ \left(\frac{1}{9} g''^2 - \frac{1}{4} g^2 - \frac{1}{4} g''^2 \right) (U_{12} U_{21} + U_{11} U_{22}) U_{23} \right. \\
& + U_{13} \left[\frac{1}{12} (g''^2 + 9g^2 + 9g'^2) U_{11} U_{12} + \left(\frac{1}{9} g''^2 - \frac{1}{4} g^2 - \frac{1}{4} g''^2 \right) U_{21} U_{22} \right. \\
& \left. \left. - \frac{5}{36} g''^2 U_{31} U_{32} + \lambda^2 (U_{21} U_{22} + U_{31} U_{32}) \right] - \frac{5}{36} g''^2 (U_{12} U_{31} + U_{11} U_{32}) U_{33} \right\} v_1 \\
& - \lambda^2 (U_{12} U_{21} U_{23} + U_{11} U_{22} U_{23} + U_{12} U_{31} U_{33} + U_{11} U_{32} U_{33}) v_1 \\
& - \left\{ \left(\frac{1}{9} g''^2 - \frac{1}{4} g^2 - \frac{1}{4} g''^2 \right) U_{13} (U_{12} U_{21} + U_{11} U_{22}) \right. \\
& + U_{23} \left[\left(\frac{1}{9} g''^2 - \frac{1}{4} g^2 - \frac{1}{4} g''^2 \right) U_{11} U_{12} + \left(\frac{4}{3} g''^2 + \frac{1}{3} g^2 + \frac{1}{3} g''^2 \right) U_{21} U_{22} \right. \\
& \left. \left. - \frac{5}{9} g''^2 U_{31} U_{32} + \lambda^2 (U_{11} U_{12} + U_{31} U_{32}) \right] - \frac{5}{9} g''^2 (U_{22} U_{31} + U_{21} U_{32}) U_{33} \right\} v_2 \\
& - \lambda^2 (U_{12} U_{13} U_{21} + U_{11} U_{13} U_{22} + U_{22} U_{31} U_{33} + U_{21} U_{32} U_{33}) v_2 \\
& + \left\{ \left[\frac{5}{36} g''^2 (U_{12} U_{13} + 4U_{22} U_{23}) - \lambda^2 (U_{12} U_{13} + U_{22} U_{23}) \right] U_{31} \right. \\
& + \left[\frac{5}{36} g''^2 (U_{11} U_{13} + 4U_{21} U_{23}) - \lambda^2 (U_{11} U_{13} + U_{21} U_{23}) \right] U_{32} \\
& \left. + \left[\frac{5}{36} g''^2 (U_{11} U_{12} + 4U_{21} U_{22} - 15U_{31} U_{32}) - \lambda^2 (U_{11} U_{12} + U_{21} U_{22}) \right] U_{33} \right\} v_3, \tag{A101}
\end{aligned}$$

$$\begin{aligned}
C_{H_2^0 H_2^0}^{H_3^0} = & \frac{1}{2} \lambda A (U_{13} U_{22} U_{32} + U_{12} U_{23} U_{32} + U_{12} U_{22} U_{33}) \\
& + \left\{ U_{13} \left[\frac{-1}{24} (g''^2 + 9g^2 + 9g'^2) U_{12}^2 - \left(\frac{1}{18} g''^2 - \frac{1}{8} g^2 - \frac{1}{8} g''^2 \right) U_{22}^2 \right. \right. \\
& + \frac{5}{72} g''^2 U_{32}^2 - \frac{1}{2} \lambda^2 (U_{22}^2 + U_{32}^2) \left. \right] + U_{12} \left[\left(\frac{-1}{9} g''^2 + \frac{1}{4} g^2 + \frac{1}{4} g'^2 \right) U_{22} U_{23} \right. \\
& \left. \left. + \frac{5}{36} g''^2 U_{32} U_{33} - \lambda^2 (U_{22} U_{23} + U_{32} U_{33}) \right] \right\} v_1 \\
& + \left\{ U_{23} \left[\left(\frac{-1}{18} g''^2 + \frac{1}{8} g^2 + \frac{1}{8} g''^2 \right) U_{12}^2 - \frac{1}{24} (16g''^2 + 9g^2 + 9g'^2) U_{22}^2 \right. \right. \\
& + \frac{5}{18} g''^2 U_{32}^2 - \frac{1}{2} \lambda^2 (U_{12}^2 + U_{32}^2) \left. \right] + U_{22} \left[\left(\frac{-1}{9} g''^2 + \frac{1}{4} g^2 + \frac{1}{4} g'^2 \right) U_{12} U_{13} \right. \\
& \left. \left. + \frac{5}{9} g''^2 U_{32} U_{33} - \lambda^2 (U_{12} U_{13} + U_{32} U_{33}) \right] \right\} v_2 \\
& + \left\{ U_{32} \left[\frac{5}{36} g''^2 (U_{12} U_{13} + 4U_{22} U_{23}) - \lambda^2 (U_{12} U_{13} + U_{22} U_{23}) \right] \right.
\end{aligned}$$

$$+ U_{33} \left[\frac{5}{72} g''^2 (U_{12}^2 + 4U_{22}^2 - 15U_{32}^2) - \frac{1}{2} (U_{12}^2 + U_{22}^2) \right] v_3, \quad (\text{A102})$$

for the neutral-scalar-Higgses;

$$\begin{aligned} C_{H^+H^-}^{H_i^0} &= \frac{-1}{4(1 + \cot^2 \beta)} \left\{ v_1(3g^2 + g'^2 - 4\lambda^2)(U_{1i} + U_{2i} \cot \beta) \right. \\ &\quad + \left(g^2 - g'^2 + \frac{4}{9} g''^2 \right) (v_1 U_{1i} \cot^2 \beta + v_2 U_{2i}) \\ &\quad + \frac{1}{9} g''^2 [v_1(v_1 U_{1i} + 16U_{2i} \cot \beta) - 5v_3(1 + 4 \cot^2 \beta) U_{3i}] \\ &\quad \left. + 4(\lambda^2 v_3(1 + \cot^2 \beta) + \lambda \cot \beta) U_{3i} \right\}, \quad (\text{A103}) \end{aligned}$$

for the charged-scalar-Higgses;

$$\begin{aligned} C_{P^0 P^0}^{H_i^0} &= \frac{v_3^2}{2(v_1^2 v_2^2 + v^2 v_3^2)} \left\{ \left[m_Z^2 \cos 2\beta - \frac{1}{9} \left(\frac{g''}{g} \right)^2 m_W^2 - \lambda^2 \frac{v_1^2 v_2^2}{v_3^2} \right] (v_1 U_{1i} + v_2 U_{2i}) \right. \\ &\quad - \lambda(v_1^3 U_{1i} + v_2^3 U_{2i}) - \lambda^2 v_3(v_1^2 + v_2^2) U_{3i} - \lambda A \frac{v_1 v_2}{v_3} (v_1 U_{1i} + v_2 U_{2i} + v_3 U_{3i}) \\ &\quad \left. + \frac{5}{36} g''^2 \left[\frac{v_1^2 v_2^2}{v_3^2} (v_1 U_{1i} + 4v_2 U_{2i} - 5v_3 U_{3i}) + v_3(4v_1^2 + v_2^2) U_{3i} \right] \right\}, \quad (\text{A104}) \end{aligned}$$

for the pseudo-scalar-Higgses, which were all extracted by plugging Eqs. (40)-(45) for the physical Higgs fields into the Higgs potential, Eq. (19).

The $H_i^0 \rightarrow \tilde{\chi}_j^0 \tilde{\chi}_k^0$, $\tilde{\chi}_j^+ \tilde{\chi}_k^-$ decay processes are quite complicated to compute. Here a simple approximation was made in which for $m_{P^0} \lesssim \mathcal{O}(500) \text{ GeV}$ its contribution to the width was 15%, otherwise 50%. This addition had a negligible affect on L^+L^- production, since $m_{P^0} = 200 \text{ GeV}$.

c. Γ_{P^0}

For the P^0 width the following processes need to be computed:

$$P^0 \longrightarrow Z_i Z_j, W^\pm H^\mp, q_i \bar{q}_i, l_i \bar{l}_i, \tilde{\chi}_i^0 \tilde{\chi}_j^0, \tilde{\chi}_i^+ \tilde{\chi}_j^-, \tilde{q}_i \tilde{q}_j^*, \tilde{l}_i \tilde{l}_j^*.$$

For $P^0 \rightarrow Z_i Z_j, W^\pm H^\mp$ the widths are zero since here $m_{P^0} < m_{Z_2}$ and $m_{P^0} \approx m_{H^\pm}$: see Figs. 6-9 and discussion therein.

The $P^0 \rightarrow q_i \bar{q}_i, l_i \bar{l}_i$ decay widths are

$$\Gamma(P^0 \rightarrow f\bar{f}) = \frac{c_f g^2}{32\pi} \left(\frac{m_f}{m_W}\right)^2 K^{fP^0}{}^2 \beta_{P^0} m_{P^0}, \quad (\text{A105})$$

via Eq. (A63), with amplitudes

$$|\overline{\mathcal{M}}_{f\bar{f}}|^2 = \frac{g^2}{2} \left(\frac{m_f}{m_W}\right)^2 K^{fP^0}{}^2 m_{P^0}^2, \quad (\text{A106})$$

where the K^{fP^0} couplings defined by Eq. (A18).

The $P^0 \rightarrow \tilde{q}_j \tilde{q}_k^*, \tilde{l}_j \tilde{l}_k^*$ decay widths are

$$\Gamma(P^0 \rightarrow \tilde{f}_j \tilde{f}_k^*) = \frac{c_f g^2 m_Z^2}{16\pi(1-x_W)m_{P^0}} K_{jk}^{\tilde{f}P^0}{}^2 \beta_{\tilde{f}_j \tilde{f}_k^*}, \quad (\text{A107})$$

via Eq. (A96), with vertex factors

$$C_{\tilde{f}_j \tilde{f}_k^*}^{P^0} = \frac{g m_Z}{\sqrt{1-x_W}} K_{jk}^{\tilde{f}P^0}, \quad (\text{A108})$$

where the $K_{jk}^{\tilde{f}P^0}$ couplings are given by Eqs. (A34)-(A38).

In this work m_{P^0} was fixed at 200 GeV . At this mass $P^0 \rightarrow \tilde{\chi}_i^0 \tilde{\chi}_j^0, \tilde{\chi}_i^+ \tilde{\chi}_j^-$ decays are suppressed [9].

REFERENCES

- [1] M.M. Boyce, **String Inspired QCD and E_6 Models**, *Ph.D. thesis (1996)*, Carleton U., Dept. of Physics, 1125 Colonel By Dr., Ottawa, ONT, Canada, K1S-5B6.
- [2] M.M. Boyce, M.A. Doncheski, and H. König, **Heavy Charged Lepton Production in Superstring Inspired E_6 Models**, *talk presentd at "MRST '96," 10th May 1996*.
- [3] Stephen Wolfram (*Wolfram Reasearch, inc: into@wri.com*), **Mathematica**, *A System for Doing Mathematics by Computer, 2nd ed, Addison-Wesley (1991)*.
- [4] JoAnne L. Hewett and Thomas G. Rizzo, *Phys. Rep.* **183**, (1989) 193.
- [5] John Ellis, D.V. Nanopoulous, S.T. Petcov and F. Zwirner, *Nuc. Phys.* **B283** (1987) 93.
- [6] J. Ellis, K. Enqvist, D.V. Nanopoulous, and F. Zwirner, *Nuc. Phys.* **B276** (1986) 14.
- [7] John Ellis, K. Enqvist, D.V. Nanopoulous, and F. Zwirner, *Mod. Phys. Lett.* **A1**, (1986) 57.
- [8] V. Barger and K. Whisnant, *Int. J. Mod. Phys.* **A3**, (1988) 1907.
- [9] J.F. Gunion, L. Roszkowski and H. E. Haber, *Phys. Rev.* **D28**, (1988) 105.
- [10] S.L. Glashow. *Nucl. Phys.* **22**, (1961),
D.J. Gross and F. Wilczek, *Phys. Rev.* **D8**, (1973) 3633,
ibid **D9**, (1974) 980,
H.D. Politzer, *Phys. Rep.* **14** (1974) 129,
S. Weinberg, *Phys. Rev. Lett.* **19**, (1967) 1264.
- [11] J.L. Rosner, **Grand Unified Theories – an Update**, *Proc. of the 2nd Lake Louise Winter Institute on New Frontiers in Particle Physics, Selected Topics in Electroweak Interactions, Chateau Lake Louise, Canada 15-21 Feb. 1897*, Eds: J.M. Cameron, B.A. Campbell, A.N. Kamal, F.C. Khanna, J. Ng, and J-M Poutissou, World Scientific

- (1987).
- [12] Graham G. Ross, **Grand Unified Theories**, *Frontiers in Physics Lecture Note Series* 60, Benjamin/Cummings (1984).
- [13] H. Fritzsch and P. Minkowski, *Ann. Phys. (NY)* **93**, (1975) 193,
R. Marshak and R. Mohapatra, *Phys. Lett.* **B91**, (1980) 222,
R.M. Mohapatra and J.C. Pati, *Phys. Rev.* **D11**, (1975) 566,
G. Senjanovic and R.N. Mohapatra, *Phys. Rev.* **D12**, (1975) 1502,
A. DeRújula, H. Georgi and S.L. Glashow. *Ann. Phys. (NY)* 109 (1977) 242, *ibid* 258.
- [14] R.N. Mohapatra, **Unification and Supersymmetry**, *The Frontiers of Quark-Lepton Physics*, Springer-Verlag (1986).
- [15] J. Wes and B. Zumino, *Nucl. Phys.* **B70** (1974) 52,
H. Haber and G. Kane, *Phys. Rep.* **117** (1985) 75.
- [16] H.E. Haber and G.L. Kane, *Phys. Rep.* **117**, (1985) 72.
- [17] H.P. Nilles, *Phys. Rep.*, **C110** (1984) 1.
- [18] L.L. Chau, *Phys. Rep.* **79**, (1981) 1,
G. Kane and M. Peskin, *Nucl. Phys.* **B195**, (1982) 29,
P. Avery, *et al.*, *Phys. Rev. Lett.*, **53** (1984) 117.
- [19] M.B. Green and J.H. Schwarz, *Phys. Lett.* **B149**, (1984) 117.
ibid **151**, (1985) 21.
- [20] Michio Kaku, **Introduction to Superstrings**, Springer-Verlag (1988).
- [21] J.L. Hewett, T.G. Rizzo and J.A. Robinson, *Phys. Rev.* **D33**, (1986) 1476.
ibid **34**, (1986) 2179.
- [22] D. London and J. Rosner, *Phys. ReV.* **D34**, (1986) 1530.

- [23] E. Cohen, *et al*, Phys. Lett. **B161**, (1985) 85.
ibid **165**, (1985) 76.
- [24] J. Rosner, Comments Nucl. Part. Phys. **15**, (1986) 195.
- [25] Vernon D. Barger and Roger J.N. Phillips, **Collider Physics**, *Frontiers in Physics Lecture Note Series*, Addison-Wesley (1987).
- [26] K.J.F. Gaemers, F. Hoogeveen, Phys. Lett. **B146**, (1984) 347.
 S.D. Willenbrock and D. Dicus, Phys. Lett. **B156**, (1985) 429.
 S. Dawson and S. Willenbrock, Nucl. Phys. **B284**, (1987) 449.
 V. Barger and W.Y. Keung, Phys. Rev. **D34**, (1987) 2902.
- [27] J.E. Cieza Montalvo, O.J.P. Éboli, and S.F. Novaes, Phys. Rev. **D46**, (1992) 181.
- [28] Ta-Pei Cheng and Ling-Fong Li, **Gauge Theory of Elementary Particle Physics**, *Oxford Science Publications*, Clarendon Press, Oxford (1986).
- [29] J.F. Gunion and H.E. Haber, Nuc. Phys. **B272**, (1986) 1.
- [30] M.M. Boyce, **Some SUSY Related Orthotoponium Phenomenology**, *M.Sc. thesis (1989)*, Avadh Bhatia Physics Laboratory, University of Alberta, Edmonton, Alberta, Canada, T6G-2J1.
- [31] H. König, Zeit. Phys. **C69**, (1996) 493.
- [32] Melvyn J. Shochet, **Physics At The Fermilab Collider**, *The Albuquerque Meeting, Aug. 2-6, 1994, The University of New Mexico, Proceedings of the 8th Division of Particle and Fields of the American Physical Society*, Ed: Sally Seidel, World Scientific (1994).
- [33] **Particle Data Group**, Phys. Rev. **D50**, (1994) 1173.
- [34] F. Abe, *et al*, Phys. Rev. Lett **74**, (1995) 2626.
 S. Abachi, *et al*, *ibid* 2632.

- [35] D. Duke and J. Owens, Phys. Rev. **D30**, (1984) 49.
- [36] J. Owens, Phys. Lett. **B266**, (1991) 126.
- [37] A.D. Martin, R.G. Roberts and W.J. Stirling, Phys. Rev. **D50**, (1994) 6734.
- [38] J.L. Hewett and T.G. Rizzo, Z. Phys. **C34**, (1987) 49.
- [39] V. Barger, T. Han, and J. Ohnemus, Phys. Rev. **D37**, (1988) 1174.
- [40] I. Hinchliffe, Int. J. Mod. Phys. **A4**, (1989) 3867.
- [41] David Griffiths, **Introduction to Elementary Particles**, John Wiley and Sons (1987).